

This article was downloaded by: [Steven W. Salisbury]

On: 28 February 2012, At: 13:09

Publisher: Taylor & Francis

Informa Ltd Registered in England and Wales Registered Number: 1072954 Registered office: Mortimer House, 37-41 Mortimer Street, London W1T 3JH, UK



Journal of Vertebrate Paleontology

Publication details, including instructions for authors and subscription information:

<http://www.tandfonline.com/loi/ujvp20>

New anatomical information on *Rhoetosaurus brownei* Longman, 1926, a gravisaurian sauropodomorph dinosaur from the Middle Jurassic of Queensland, Australia

Jay P. Nair ^a & Steven W. Salisbury ^{a b}

^a School of Biological Sciences, The University of Queensland, Brisbane, Queensland, 4072, Australia

^b Section of Vertebrate Paleontology, Carnegie Museum of Natural History, 4400 Forbes Avenue, Pittsburgh, Pennsylvania, 15213-4080, U.S.A.

Available online: 28 Feb 2012

To cite this article: Jay P. Nair & Steven W. Salisbury (2012): New anatomical information on *Rhoetosaurus brownei* Longman, 1926, a gravisaurian sauropodomorph dinosaur from the Middle Jurassic of Queensland, Australia, *Journal of Vertebrate Paleontology*, 32:2, 369-394

To link to this article: <http://dx.doi.org/10.1080/02724634.2012.622324>

PLEASE SCROLL DOWN FOR ARTICLE

Full terms and conditions of use: <http://www.tandfonline.com/page/terms-and-conditions>

This article may be used for research, teaching, and private study purposes. Any substantial or systematic reproduction, redistribution, reselling, loan, sub-licensing, systematic supply, or distribution in any form to anyone is expressly forbidden.

The publisher does not give any warranty express or implied or make any representation that the contents will be complete or accurate or up to date. The accuracy of any instructions, formulae, and drug doses should be independently verified with primary sources. The publisher shall not be liable for any loss, actions, claims, proceedings, demand, or costs or damages whatsoever or howsoever caused arising directly or indirectly in connection with or arising out of the use of this material.

NEW ANATOMICAL INFORMATION ON *RHOETOSAURUS BROWNEI* LONGMAN, 1926, A GRAVISAURIAN SAUROPODOMORPH DINOSAUR FROM THE MIDDLE JURASSIC OF QUEENSLAND, AUSTRALIA

JAY P. NAIR^{*1} and STEVEN W. SALISBURY^{1,2}

¹School of Biological Sciences, The University of Queensland, Brisbane, Queensland, 4072, Australia, jayraptor@gmail.com;

²Section of Vertebrate Paleontology, Carnegie Museum of Natural History, 4400 Forbes Avenue, Pittsburgh, Pennsylvania 15213-4080, U.S.A., s.salisbury@uq.edu.au

ABSTRACT—*Rhoetosaurus brownei* is the only known named pre-Cretaceous sauropod from Australia. It is therefore a potentially important taxon for understanding global paleobiogeographic and phylogenetic patterns among early sauropods. Despite its obvious significance, *Rhoetosaurus* has been too poorly understood to be included in most recent analyses of early sauropod evolution. With this in mind, we evaluated the osteology and phylogeny of undescribed materials of *Rhoetosaurus*, in order to attempt to close the gap in this understanding. The lower hind limb of *Rhoetosaurus* highlights a plethora of differences from other sauropods, supporting the distinctiveness of *Rhoetosaurus* even in the absence of other materials. Some unique traits include prominent crests and sulci on the tibia medially, a narrow metatarsal articular bridge, and pedal claws with an accessory groove or fossa. The pes plesiomorphically retains four claws where most sauropods have three, and bears superficial similarity to that of *Shunosaurus*. Preliminary cladistic analysis confirms that *Rhoetosaurus* is a non-neosauropod gravisaurian, although weak support for the most parsimonious topology suggests further findings are required to improve upon incompleteness in the character data. Examination of alternative phylogenetic hypotheses rules out a close relationship between *Rhoetosaurus* and East Asian Jurassic sauropods, and indicates a closer examination of the potential relationships between *Rhoetosaurus* and other contemporaneous Middle Jurassic Gondwanan sauropods is necessary.

INTRODUCTION

Sauropod dinosaurs are becoming an increasingly recognized constituent of Cretaceous terrestrial faunas of Queensland, Australia (Coombs and Molnar, 1981; Molnar and Salisbury, 2005; Salisbury et al., 2006; Hocknull et al., 2009); however, the pre-Cretaceous record of this group in Australia is scant. *Rhoetosaurus brownei* is known from a single partial skeleton from Middle Jurassic strata near Roma, Queensland (Longman, 1926), and is one of only two named dinosaurs from pre-Cretaceous times in Australia (the other is *Ozraptor* Long and Molnar, 1998).

Overall, little is known about the dinosaurian faunas that inhabited Australia before Cretaceous times. Apart from *Rhoetosaurus*, current knowledge of pre-Cretaceous Australian dinosaurs consists of a handful of mostly scanty skeletal fossils (Long, 1992; Grant-Mackie et al., 2000) and a slightly higher diversity of trackways (Bartholomai, 1966; Thulborn, 1994, 2000). The extensive gaps that exist in the record of Australian pre-Cretaceous dinosaurs have resulted in a deficiency in our understanding of their evolution and paleogeography. Given this poor representation, *Rhoetosaurus* holds great potential in addressing such queries. However, the most recent descriptions of *Rhoetosaurus* are 80 years old (Longman, 1926, 1927a, 1927b, 1929), and a reappraisal of this taxon is overdue considering recent advances in the understanding of sauropod phylogeny.

This research details the osteology of the previously undescribed right hind limb of *Rhoetosaurus* (Rich and Vickers-Rich, 2003), a specimen that includes an almost complete pes (first depicted in Molnar, 1991). Using these new data, we re-evaluate the position of *Rhoetosaurus* in sauropod phylogeny, as well as briefly consider pedal evolution and functionality in sauropods.

Historical Overview

In early 1924, a passing stockman chanced upon the type material of *Rhoetosaurus brownei* on Durham Downs Station (now Taloona Station, following subdivision), Roma Shire, southwest Queensland (Fig. 1; Longman, 1926; Rich and Vickers-Rich, 2003). The find was reported to Longman at the Queensland Museum, who named and described *Rhoetosaurus* in 1926, and added further details a year later (Longman, 1926, 1927a). The original material, comprising a series of weathered thoracic and caudal vertebrae, and fragments of the pelvis, was found buried under soil on a gully bank. Following Longman's suggestion that further bones from the same animal were likely to be present (Longman, 1927a:1; Thulborn, 1985), teams from the Queensland Museum and The University of Queensland returned to further prospect the original locality in 1975. An almost complete right crus, astragalus, and pes were recovered in 1976. Teams from Latrobe University, Melbourne Museum, and the University of Queensland continued to visit the locality on an irregular basis from the early 1980s to the present. From these trips, a cervical vertebra and ribs were recovered (Rich and Vickers-Rich, 2003; pers. observ.). The sum of material to date forms a significant portion of a single skeleton, which represents the most complete pre-Cretaceous dinosaur known from Australia.

Materials and Terminology

Institutional Abbreviations—AMNH, American Museum of Natural History, New York, New York, U.S.A.; CM, Carnegie Museum of Natural History, Pittsburgh, Pennsylvania, U.S.A.; FMNH, Field Museum of Natural History, Chicago, Illinois, U.S.A.; QM, Queensland Museum, Geoscience collection, Brisbane, Queensland, Australia; UQ, University of Queensland, Brisbane, Queensland, Australia; USNM, National Museum of

*Corresponding author.

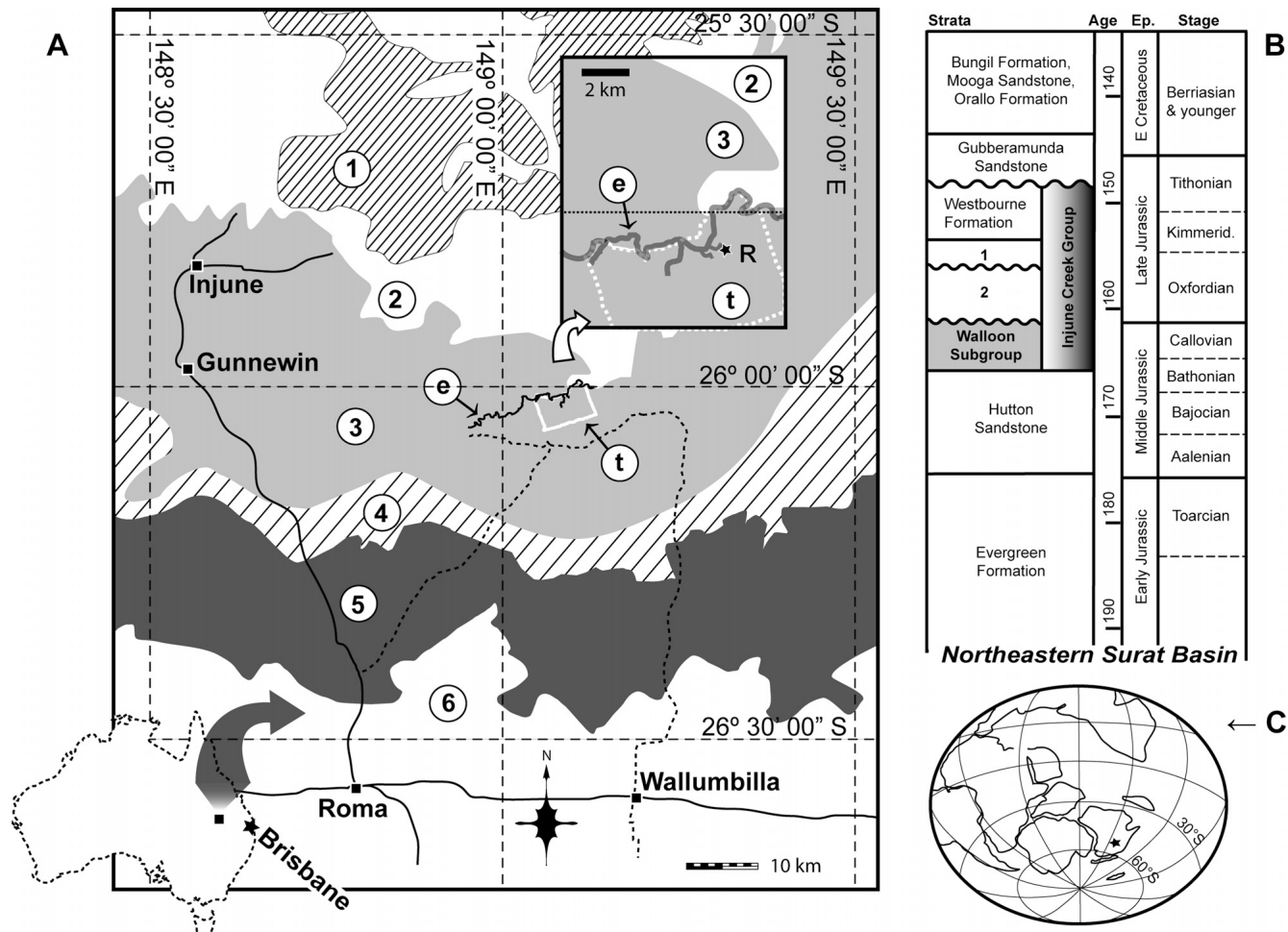


FIGURE 1. Geographic, stratigraphic, and paleogeographic context of the type location of *Rhoetosaurus brownei*. **A**, map of the northeastern Surat Basin, showing outcrops. **Abbreviations:** 1, Evergreen Formation; 2, Hutton Sandstone; 3, Walloon Coal Measures (= Walloon Subgroup; coeval with the Birkhead Formation of the Eromanga Basin); 4, Springbok Sandstone and Westbourne Formation; 5, Gubberamunda Sandstone; 6, post-Gubberamunda Sandstone succession. The enlarged insert refers to the type locality of *Rhoetosaurus* (designated by **R**), and occurs adjacent to Eurombah Creek (**e**) within Taloona Station (**t**). **B**, Jurassic-Early Cretaceous lithostratigraphic units in Surat Basin indicated on map (**A**), with ages and correlated stages. **Abbreviations:** 1, Springbok Sandstone; 2, hiatus (coeval with the Adori Sandstone of the Eromanga Basin). **C**, paleogeographic location of Surat Basin (star) during the Middle Jurassic (modified from Grant-Mackie et al., 2000).

Natural History, Washington, D.C., U.S.A.; **YPM**, Yale Peabody Museum, Yale University, New Haven, Connecticut, U.S.A.

Materials—The right lower hind limb elements of QM F1659, the tibia, fibula, astragalus, and pes, were studied firsthand. The right pes was replicated at UQ, from which we complemented our observations of the specimens (see Supplementary Data [available online at www.tandfonline.com/UJVP] for measurements of QM F1659).

Anatomical Terminology—Excluding the autopodia, the orientations, directions, and surfaces of appendicular bones are described with the following paired opposing terms: proximal/distal, cranial/caudal (sensu front/back), and lateral/medial. As common for describing sauropod autopodia specifically (e.g., Upchurch et al., 2004a), dorsal/plantar is used in place of cranial/caudal in relation to the bones of the feet, which interact with the substrate, and are therefore naturally positioned unlike other long bones.

SYSTEMATIC PALEONTOLOGY

SAURISCHIA Seeley, 1887

SAUROPODOMORPHA von Huene, 1932, sensu Galton and Upchurch, 2004

SAUROPODA Marsh, 1878, sensu Wilson, 2005

GRAVISAUROidea Allain and Aquesbi, 2008

RHOETOSAURUS BROWNEI Longman, 1926

(Figs. 2–14)

Hypodigm—The syntype series (described in Longman, 1926) plus referred specimens (Longman, 1927a; Rich and Vickers-Rich, 2003) are all assigned to QM F1659. The hypodigm comprises at least 40 vertebrae, including two cervical corpora, at least five thoracic vertebrae, five partial thoracic ribs, an incomplete sacrum, a continuous sequence of 22 caudal vertebrae, associated hemal arches, fragments of the ilia, an ischium, the left and right pubic bones, and the right hind limb elements: femur, tibia, fibula, astragalus, and pes, all in addition to in excess of hundreds of fragments and blocks, many of which await preparation. Materials described after 1926, including the hind limb skeleton covered in this research, are technically considered referred specimens (not part of the type series syntypes), because these were excavated and described subsequent to the original description (Article 72.1.2 in International Commission on Zoological Nomenclature, 1999). However, most, if not all, of the referred material is from the same individual as the syntype

described by Longman in 1926, based on non-overlap of body parts, provenance from a spatially restricted field site, and degree of taphonomic articulation suggestive of a single skeleton (see below).

Type Locality—On the slope of a shallow gully within ‘block 1v’ (Longman, 1926; Strong, 2005), draining into the south side of Eurombah Creek, Taloola Station (originally part of Durham Downs Station), ~60 km NNE of Roma, southwestern Queensland (Fig. 1A).

Horizon and Age—Walloon Coal Measures (WCM, = ‘Walloon Subgroup’), Injune Creek Group, Surat Basin. The material derives from the lowermost section of the Walloon Coal Measures (preceding increased intercalated coal bands). The name ‘Eurombah Formation’ has been applied to this section locally near the type locality (Swarbrick et al., 1973), but this unit is not widespread and cannot be consistently distinguished from the WCM in other parts of the Surat Basin (Green et al., 1997). The age of the lowermost WCM, based on palynostratigraphy (Helby et al. [1987], *Contignisporites cooksoniae* Oppel Zone; McKellar [1998], *Contignisporites glebulentus* Interval Zone) is late Bathonian–middle Callovian (Fig. 1B).

Paleoenvironment—Paleogeographic reconstructions posit that present day southwestern Queensland lay within a latitude of 40–60°S during Middle Jurassic times (Fig. 1C; Rich, 1996; Rich et al., 2002). The climate for the region was a warm to warm-temperate moist one, based on palynological, micro-, and megafloral records (summarized in McKellar, 1998). The depositional setting was mostly coal swamps for the WCM, with the ‘Eurombah Formation’ component laid down rapidly under fluvial or overbank conditions (Green et al., 1997).

Revised Diagnosis—Non-neosauropod sauropod characterized by the following autapomorphies (A), unique combination of clade synapomorphies (S), and plesiomorphies (P): tibia having multiple distal crests and sulci medially (A); concentric proximal fossa present on medial surface of tibia (A); lateromedial dimension of distal tibia forms its greatest breadth (S: Neosauropoda); mid-lateral surface of fibula osteologically featureless, lacking tubercle or scar (A); proximal and distal surfaces of astragalus sub-parallel (?A, also *Ohmdenosaurus lasicus*); proximal articular surfaces of metatarsi elliptical and narrow dorsoplantarly (A, also to a lesser extent in *Shunosaurus li*); metatarsi bearing distally situated crista on lateral side; (?S: irregularly distributed amongst Eusauropoda); distal part of metatarsal I twisted laterodorsally relative to proximal end (S: Neosauropoda); prominent crest and apical process developed on medial side of cranial face of metatarsal II (A, lesser developed ridges also in diplodocids); second phalanx of digit II triangular in dorsal outline (A); lateral crest on first phalanx of digit IV (A); proximal articular facets of unguals angled due to medial surface extended further proximally than lateral counterpart (?A); accessory fossa or groove developed on medial face of pedal unguals (A); pes retaining at least four unguals (P: not *Omeisaurus* spp. + more-derived Sauropoda).

Comments

Degree of Articulation and Taphonomic Implications—Archival site excavation information from the 1920s and 1970s is sparse. Longman (1926, 1927a) indicated in his description of the syntype material that part of it was semi-articulated. A photograph taken ca. 1926, published in Longman (1927b), shows an exposed series of articulated vertebrae *in situ*. In repository (QM), signs of former articulation in the field are evident in the material. Most thoracic and caudal vertebral blocks comprise two adjoining faces: the caudal half of a preceding vertebra in contact with the cranial half of the succeeding element. Caudal hemal arches are closely associated with their respective vertebral bod-

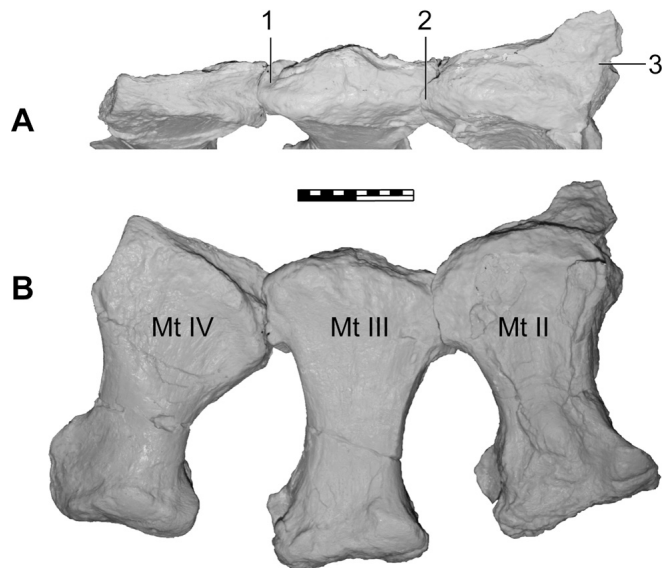


FIGURE 2. Assembled casts of the metatarsi II–IV of *Rhoetosaurus brownii*, illustrating the original close taphonomic (and presumably *in vivo*) articulation between the bones in **A**, proximocranial; **B**, cranial views. **1**, likely fragment of Mt-IV adherent on Mt-III (see text); **2**, jigsaw fit of matrix between Mt-II and Mt-III; **3**, matrix, originally adherent to Mt-I in the field. Scale bar equals 10 cm.

ies. The lower hind limb was in articulation during its excavation, based on Wade’s informal account of the excavation during which it was discovered (cited in Rich and Vickers-Rich, 2003). Several metatarsal and phalangeal bones are currently articulated, or were joined by matrix until recently. Before preparation, the metatarsi were bridged by matrix proximally, resulting in them being in close connection to one another (Fig. 2). This preservational configuration reveals the metatarsus is (1) slender and linear in proximal view, and (2) splayed outwards from the tarsus (Fig. 2). If taphonomic articulation reflects natural anatomy, then it has implications for the overall posture of the foot as well as biomechanics of its component parts.

One or Two Individuals?—Longman (1927a:1) noted the remains were scattered in “soil over an area of several yards,” which taken with the observation that no overlap between any of the elements is seen, is suggestive of a single, once articulated skeleton. We consider the excavations in 1975–1976 identified additional hypodigm material from the same individual from the original type locality because at least one bone fragment “fitted [perfectly with] a piece” recovered from the 1925–1926 excavations (the right tibia, unpublished QM staff correspondences; Rich and Vickers-Rich, 2003:49–50). Claims that the meagre remains recovered in 1982 and post-1995 represent an individual from a different locality (Rich and Vickers-Rich, 2003:53; T. Rich, pers. comm. and unpubl. field notes) have no bearing on the association of the syntype and its referred constituent (all pre-1982 discoveries). They do, however, have some implication for the distribution and abundance of the rare pre-Cretaceous sauropod component in eastern Australia. Part of the rationale for a two-site argument is that the sites were suggested to differ in surface geomorphology when photos of the area from different times were compared (i.e., Longman, 1927b:98; Rich and Vickers-Rich, 2003:50–52). However, as part of a gully that drains into the Eurombah Creek, considerable erosion has taken place at the locality since the time of Longman’s photos. When the original specimen was found in 1923, it was very close to a large ironbark on a

gentle slope that led down to Eurombah Creek (N. Timms, pers. comm., 22 August 2002). Since that time, parts of this paddock have been bulldozed, and the ironbark and other trees have been removed, facilitating further erosion of the gully. In the absence of precise collection data revealing otherwise, we advise considering all of the known material to represent one skeleton from a single site, which over the course of 85 years has altered appreciably with natural and human-induced processes.

DESCRIPTION

Preservation

Of the right hind limb, every region is represented. The femur, lacking its distal end, has already been described (Longman, 1927a), and will not be considered here. The crus is complete but segregated into three blocks. The first is the conjoined (by matrix) proximal ends of the tibia and fibula. The other two are the diaphyses plus distal epiphyses of the tibia and fibula, respectively. The tarsus is represented only by the astragalus—a calcaneum having not been recovered if ossified in *Rhoetosaurus*. The recovered pes lacks digit V, but otherwise includes a full complement of metatarsi, non-terminal phalanges, and unguals for digits I–IV.

Inconsistent lithology in the matrix surrounding the bones has made it difficult to ascertain the details of some the elements (also see comment by T. Thulborn, in Rich and Vickers-Rich, 2003). The matrix includes calcareous-ferruginous sandstone, clay-ironstone, and mudstone. As also noted by Longman (1926, 1927a), a closely adhering calcareous cement is difficult to remove and proves difficult to distinguish from the contours of the bones. This is especially true around the astragalus, both ends of the tibia, and on some metatarsi; the latter are also covered extensively with restorative agents. We point out where specific instances of preservation obscure osteological details in the subsequent description.

Crus

The proximal articular surface of the conjoined crus is deformed such that the region is declined laterally (Fig. 3C–D). The medial surface of the proximal fibula is obscured by adherent matrix and the tibia. Viewed caudally here (Fig. 3D), the matrix has resulted in poor demarcation of the fibula from the tibia.

Tibia—The right tibia (Figs. 3–4) is 65% of the length of the preserved portion of the femur, and is stouter than the latter bone both proximally and distally. Overall it is weakly bowed owing to the shaft arching medially away at the proximal region. Furthermore, it is twisted about its long axis by means of gentle caudolaterally directed torsion of the distal half (and associated tarsus), relative to the proximal extremity.

The tibial head has a roughly concentric planar proximal articular surface that is declined laterally. It is slightly broader craniocaudally than transversely. A low and simple tabular cnemial crest projects laterally but not more than the extent of the fibula. The base of the cnemial crest arises from the shaft no more than 30% distal to the proximal articular face. The crest is thickest proximally and tapers toward the base. On the opposite surface (craniomedial) of the tibial head a tear-shaped sulcus is present (Fig. 3B). The sulcus appears shallow but its depth is difficult to estimate with the infill of matrix. Proximal to this feature, the tibial head is flared medially into a short shelf-like process. On the opposite side, a faint broad caudomedial ridge originates proximally but grades into the shaft.

The shaft is relatively unremarkable. The proximal break indicates a slightly reniform cross-section. At this point the shaft is twice as thick craniocaudally than lateromedially. Distally, the shaft expands mediolaterally to assume a triangular form in transverse cross-section.

The greatest breadths of the tibia are observed distally, with the craniocaudal width only slightly less than lateromedial measurement. A lateral expansion of the distal tibia forms a smooth

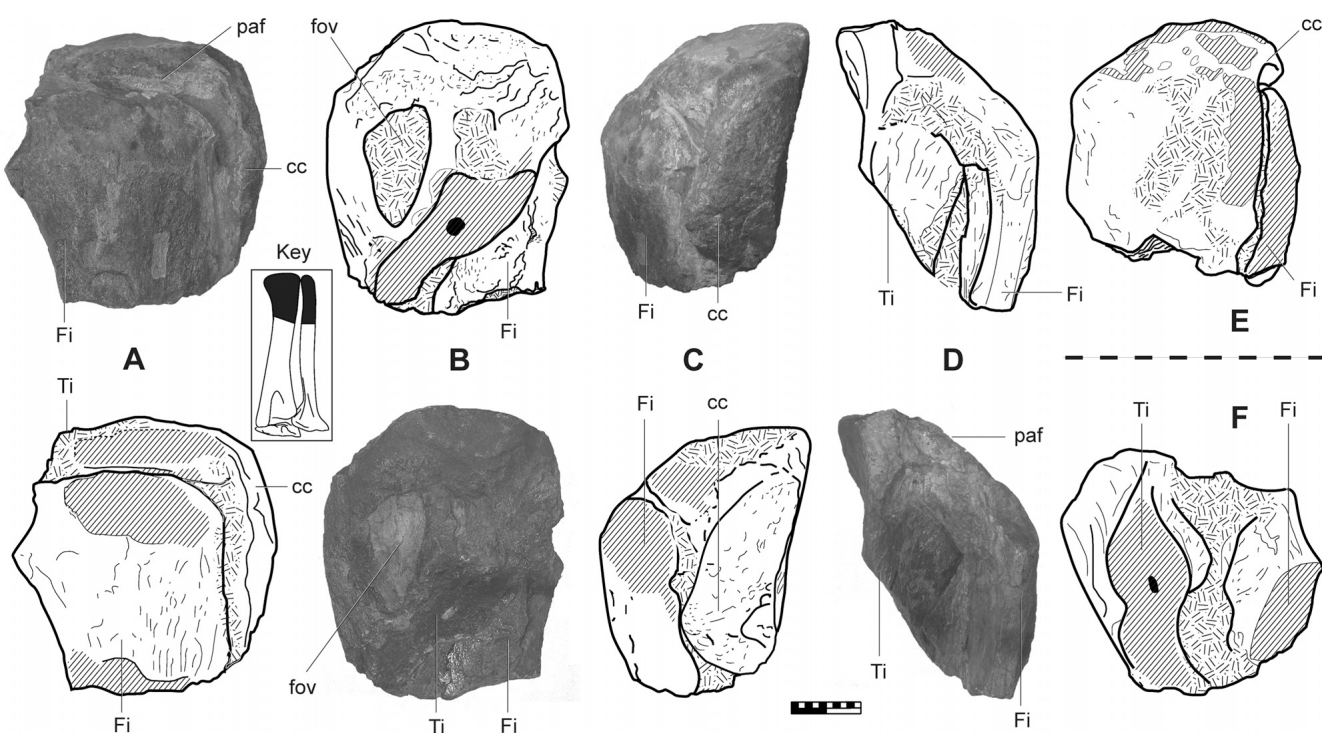


FIGURE 3. Proximal end of the conjoined right fibula and tibia of *Rhoetosaurus brownei*. **A**, lateral; **B**, medial; **C**, cranial; **D**, caudal; **E**, proximal; **F**, distal (break) views. Abbreviations: **cc**, cnemial crest; **Fi**, fibula; **fov**, fovea; **paf**, proximal articular face; **Ti**, tibia. Key shows outline of crus-tarsus (caudal view), specimen indicated in black. Scale bar equals 10 cm.

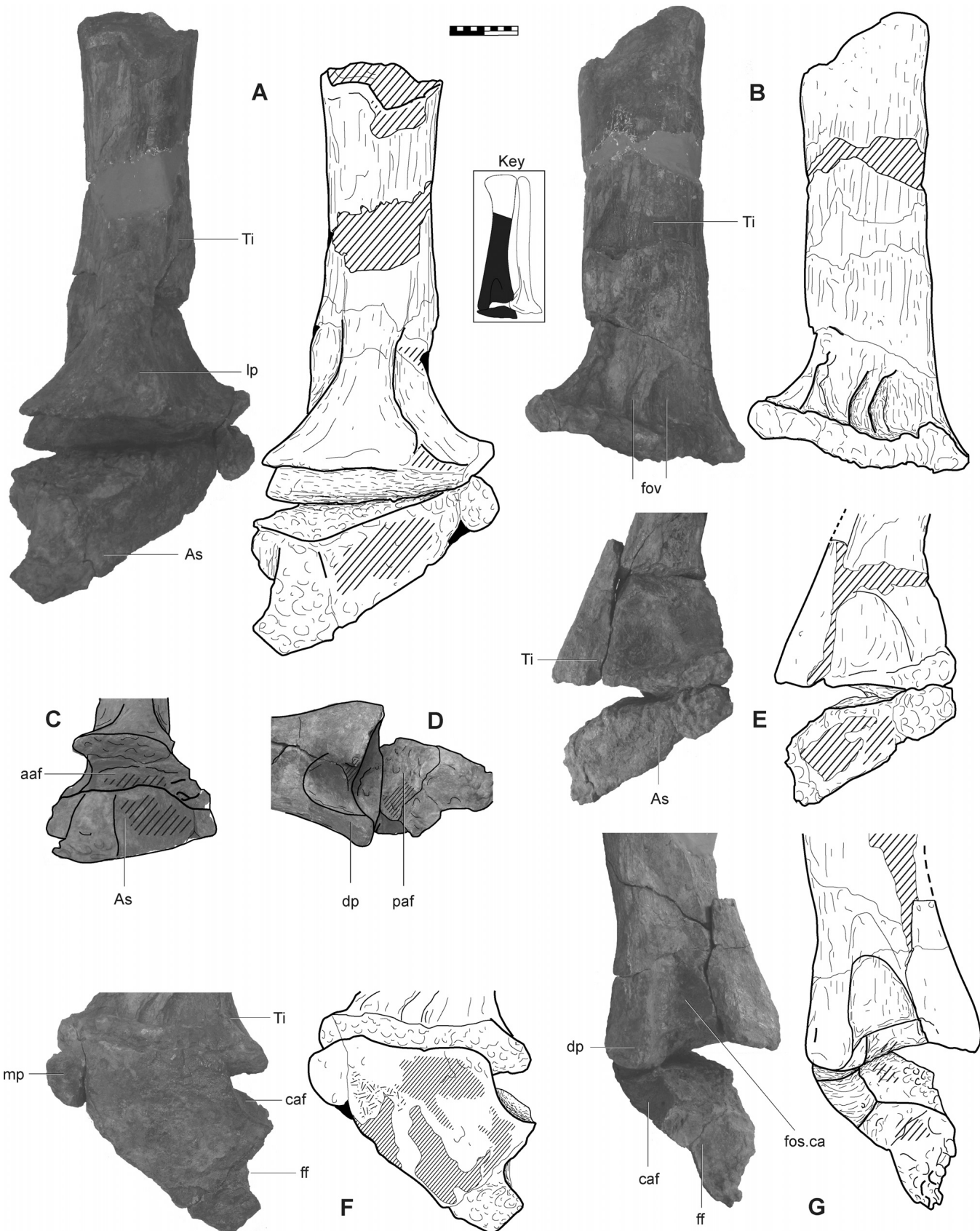


FIGURE 4. Shaft and distal end of tibia, and close up of adherent astragalus of *Rhoetosaurus brownii*. **A**, lateral; **B**, medial; **C**, distolateral views; **D**, oblique caudoproximal focus on astragalus; **E**, cranial; **F**, distal; **G**, caudal views. Abbreviations: **aaf**, astragalar articular facet; **As**, astragalus; **caf**, caudal astragalar fossa; **dp**, descending process; **ff**, fibula facet; **fos.ca**, caudal fossa; **lp**, lateral process; **mp**, medial process; **paf**, proximal articular face; **Ti**, tibia. Key shows outline of crus-tarsus (caudal view), specimen indicated in black. **C–D** not to scale, otherwise scale bar equals 10 cm.

bulge that is received in the adjoining medial fossa of the fibula. The caudomedial corner of the articular face extends distally to form a protuberance. Between this, the descending process, and the lateral bulge, the caudal face is excavated into a smoothly arched fossa (Fig. 4G). This fossa is bounded at its deepest point medially by a broad caudomedial ridge that extends proximally from the descending process. The medial margin of the distal articular facet forms a rounded rim, which has a rugose surface that is approximately 30 mm thick. Immediately proximal to this prominence, the face of the tibia is depressed but marked by a series of shallow but prominent crests (Fig. 4B). Two of the crests are arched caudally, are parallel, and bound smaller and deeper depressions. The distomedial rim extends cranially around the perimeter of the distal tibia, where, at the craniomedial bend, it is comparatively thicker and more rugose, but then narrows laterally. The cranial surface of the tibia above the rim is slightly depressed and smooth. The distal articular surface is uneven and variably pitted (Fig. 4C).

Fibula—The fibula (Figs. 3, 5) is 105% the length of the tibia (see measurements in Supplementary Data), thus extending distally beyond the tibia. It is comparatively slender due to it being much less expanded at the extremities and having a more cylindrical shaft. The proximal end is barely expanded craniocaudally and rather flattened mediolaterally, yielding an elliptical proximal surface. In caudal view (Fig. 5D), the lateral flaring of the distal end gives the fibula a marginally sigmoidal shape, something that is also exaggerated by deformation of the proximal end medially. Although the proximal medial face is obscured by matrix, a low rounded base of what is likely the tibial tuberculum is suggested. Away from the proximal end the shaft face becomes smoother. It is also mediolaterally broader around this mid-section. A large trapezoid fossa occupies the distal two-fifths of the medial surface, but is more pronounced on the cranial half, where it is deeper (Fig. 5B). Except for the weakly striated preservation of the surface, the lateral face is anatomically featureless. The distal end is expanded in all orientations, particularly toward the caudolateral and craniomedial corners. As in the tibia, the perimeter around the distal surface is developed into a rugose rim, which is particularly flared distal to the medially situated trapezoid fossa. An ovoid distal articular facet is rugose (Fig. 5E).

Tarsus

Re-orientation of the Astragalus—The interpretive morphology of the astragalus is problematic due to its poorly preserved condition. Assuming the astragalar margins have been correctly interpreted, this bone is about 80–90% complete. The astragalus appears to have undergone some degree of rotation, post mortem, which if not accounted for, would render a description of its morphology pointless where comparisons are made with other sauropod astragali. The astragalus is adhered to the distal face of tibia medially, suspended from the distomedial tibial edge (Figs. 4, 6A), and so obscures areas of both the distal tibia and proximal astragalus. The astragalus, therefore, should be rotated proximally, using the distomedial edge of the tibia as a hinge. Even reconciling this, the astragalus remains craniocaudally broad but lateromedially narrow (Fig. 6A). This form is incomparable with other saurischians, such as the phylogenetically bracketed exemplars *Saturnalia tupiniquim* (Fig. 6B), *Apatosaurus ajax* (Fig. 6C), and *Camarasaurus grandis* (Fig. 6D). In these, and all other saurischians, the astragalus is lateromedially longer than craniocaudally, thus implying a requirement for rotation about the proximodistal axis. When viewed distally, clockwise rotation of the astragalus by 30–40° reconciles several previously anomalous features of the astragalus in *Rhoetosaurus* with traits observed for other sauropods, approximately in their typical orientations. The result (Fig. 6E) is utilized in the descrip-

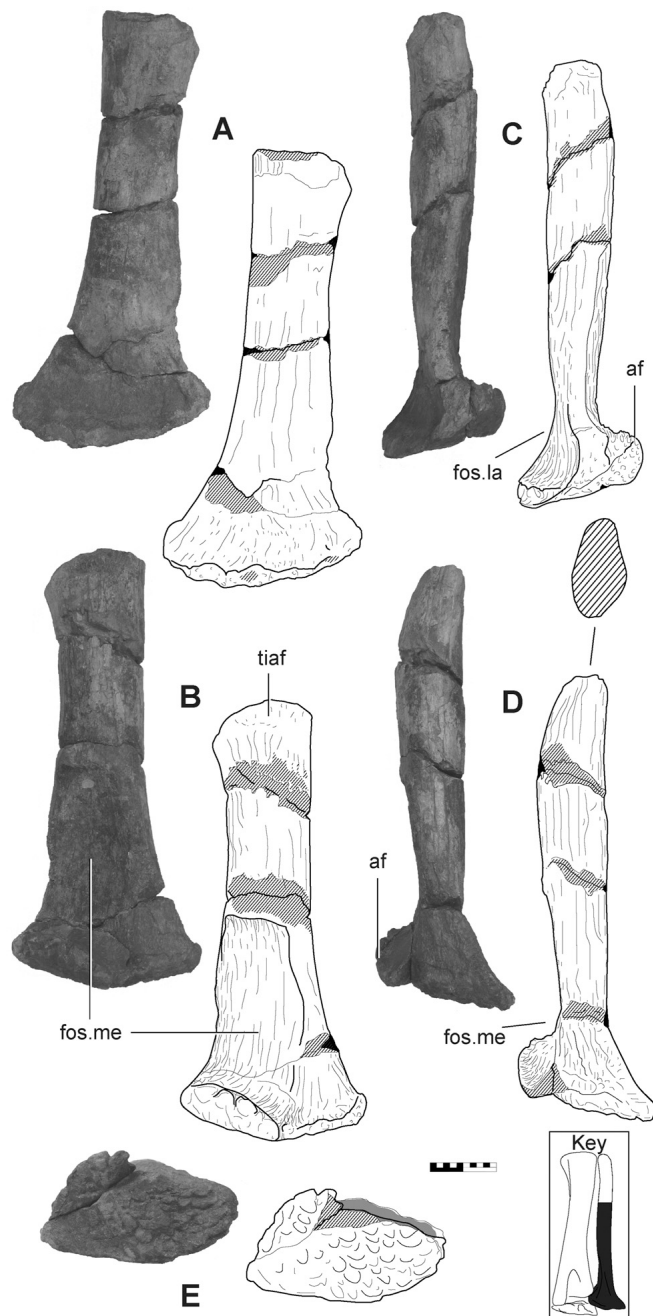


FIGURE 5. Shaft and distal end of right fibula of *Rhoetosaurus brownrei*. **A**, lateral; **B**, medial; **C**, cranial; **D**, caudal; **E**, distal views. Abbreviations: **af**, astragalar facet; **fos.la**, distal lateral depression; **fos.me**, distal medial fossa; **tiaf**, tibial articular face. Key shows outline of crus-tarsus (caudal view), specimen indicated in black. Scale bar equals 10 cm.

tion below as the orientation (relative to the tibia) in which the osteological landmarks of the astragalus are deciphered.

Description of the Astragalus—The astragalus is a flattened angular element with irregular surface texture (Figs. 4E, 6). In distal aspect, the astragalus narrows medially, due to its triangular distal outline. The medially tapering projection of the distal outline was previously called the ‘internal projection’ by Bonaparte et al. (2000) and ‘medial apex’ by Bonnan (2005), but is more precisely described as a medial process. The medial process

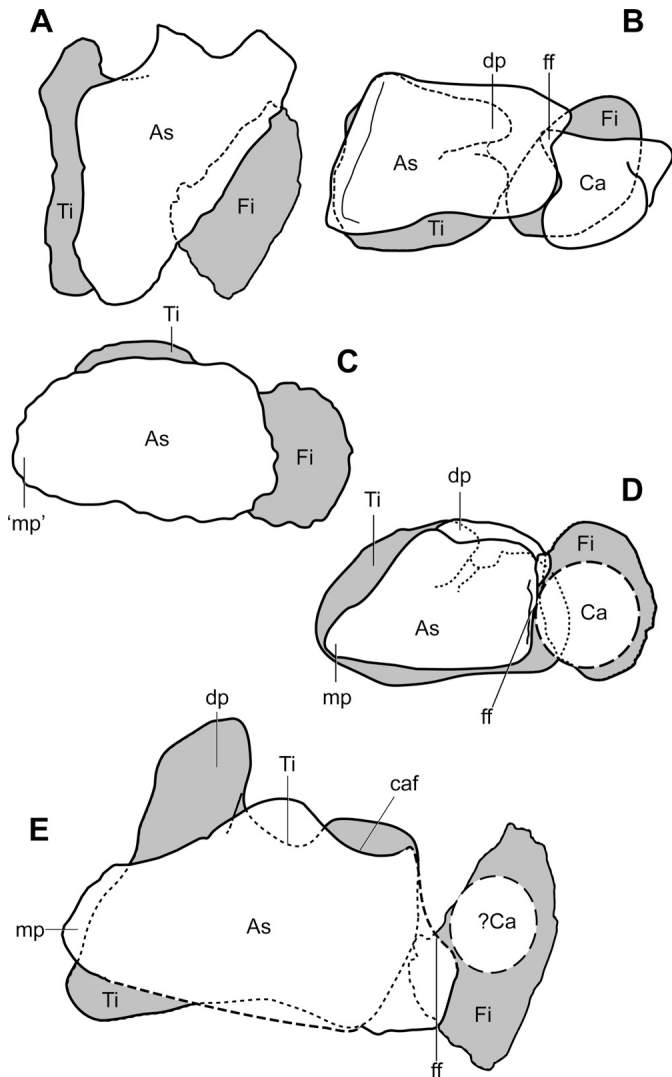


FIGURE 6. Reconstruction of sauropodomorph crus and tarsi in distal view. **A**, *Rhoetosaurus brownii* as currently preserved (astragalus adherent to the tibia, with fibula emplaced); **B**, *Saturnalia tupiniquim* (distal tarsal bones omitted); **C**, *Apatosaurus ajax*; **D**, *Camarasaurus grandis*; **E**, *Rhoetosaurus brownii* as interpreted, corrected for rotation of astragalus; calcaneum hypothetical. In all depictions, crus elements are in grey tone and upper tarsal bones are in white; medial is to the right and cranial toward the bottom. *Saturnalia* modified from Langer (2003); *Apatosaurus ajax* taken from Upchurch et al. (2004b); *Camarasaurus grandis* is based on YPM 1905 (modified from Ostrom and McIntosh, 1966), which is preserved without a calcaneum, although other *C. grandis* specimens preserve calcanea (Bonnan, 2000). **Abbreviations:** **As**, astragalus; **caf**, caudal astragalar fossa; **Ca**, calcaneum; **dp**, descending process; **Fi**, fibula; **ff**, fibula facet; **fos.ca**, caudal fossa; **mp**, medial process; **Ti**, tibia. Not to scale.

concomitantly represents the proximodistally most constricted region of the astragalus, because in cranial view the astragalus is trapezoid-shaped, thus also narrowing medially. The distal articular surface is entirely flat, though it is unclear how much of this is due to incompleteness. The proximal face is similarly sub-planar, and lacks indication of an ascending process. A fossa, present caudally, is unlike the remaining exposed astragalus in its marked smoothness. This fossa, the caudal astragalar fossa (Figs. 4G, 6E), is relatively short, occupying 35% of the lateromedial length of the astragalus, and is simple in its construction. Meeting

the caudal fossa laterocaudally at a narrow crest is another fossa, here interpreted as a fibula facet, primarily due to its lateral proximity. This articulation for the fibula is an abraded and shallow concavity that is directed slightly laterocaudally (increased lateral orientation is gained with a greater degree of rotation of the astragalus). The fibula facet is 50% the craniocaudal length of the astragalus. Laterally, it terminates at a rounded and rugose craniolateral prominence. The cranial face is rugose, as it extends linearly from that craniolateral corner to the medial process (Fig. 4E–F).

Pes

Metatarsal I—The first metatarsal (Fig. 7) is approximately quadrangular in outline when viewed in dorsal aspect, being longer proximodistally than lateromedially. It is gently twisted about the long axis such that the medial epicondylar area wraps laterally, in addition to arching dorsally at both the proximal and distal extremities. The proximal surface is slightly declined medially, and is roughly triangular in form. One of the apices of the triangular outline is directed plantarly, whereas the other two corners represent medial and lateral proximal points, both of which extend distally to their respective condyles along relatively narrow medial and lateral faces. The distal half of the dorsal face is excavated. Broad medial and lateral longitudinal crests and an expansion of the distal epicondyloid plantarly bound a similar but larger sulcus on the plantar face. Between the proximal articular face and the distal epicondyloid region, the medial surface is twice as narrow as its lateral counterpart. Distally, it expands into a medial condyle, which although capped by a large projection of matrix, appears simple. In contrast, the lateral condyle is inclined to face distoplantarly and is more expanded than its medial counterpart, expanding proximally in an extension that also flares laterally. On the lateral surface, a small shallow fossa is housed in the space dorsal to the lateral condyle, adjoining the laterodistal process. The intercondylar region, although partly obscured by cemented matrix between the condyles, is concave plantodistally.

Metatarsal II—The remaining metatarsi, which are discernibly longer than Mt-I, are sub-equal in overall form and length. Of these, Mt-II (Fig. 8) is the largest, its shaft being twice as stout as the shafts of Mt-III and Mt-IV. Despite matrix and restorative agents encasing much of the proximal region, Mt-II is notably marked by discrete paired longitudinal crests both dorsally and plantarly. The medial crest on the dorsal face, in particular, expands proximally to form a strong process (Fig. 8E). On the plantar surface, the medial ridge deviates strongly medially. Mt-II is crescent-like in proximal view, and the proximal face is convex in dorsal aspect. The distal section is expanded in all directions more so than the proximal surface. The distal epicondyloid region of Mt-II is separated into medial and lateral condyles by a shallow intercondylar groove. Plantarly, the groove becomes deeply incised away from the distal articular surface. Both distal regions of the medial and lateral faces have shallow fossae, yet the medial face proximal to the roller-shaped condyle is simpler than its lateral counterpart. On the lateral face, a short plantarly situated crest arises as a proximally directed extension of the condyle (Fig. 8B). Mt-II, as well as metatarsi III–IV, has a distal articular surface that is more rugose than its proximal surface, especially along the plantar area.

Metatarsal III—Metatarsi III and IV are compressed relative to the preceding metatarsi, each bearing shaft breadths that are 3 times longer lateromedially than dorsoplantarily. At their proximal ends, both bones are similarly expanded lateromedially but not dorsoplantarily. The more robust element, Mt-III (Fig. 9), has a proximal articular area greater than the other metatarsi with the exception of Mt-I. A medially situated low ridge emerges below the proximal articular surface on the dorsal face of Mt-III. This

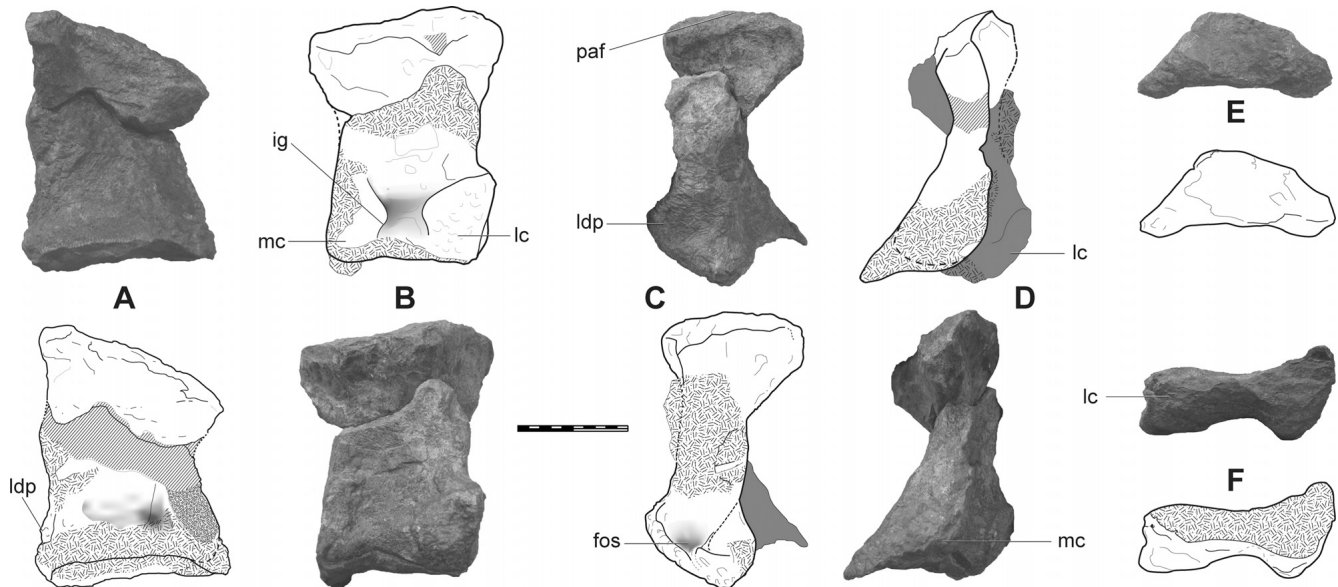


FIGURE 7. Metatarsal I of *Rhoetosaurus brownei*. **A**, dorsal; **B**, plantar; **C**, lateral; **D**, medial; **E**, proximal; **F**, distal views. Abbreviations: **fos**, fossa; **ig**, intercondylar groove; **lc**, lateral condyle; **ldp**, laterodistal process; **mc**, medial condyle; **paf**, proximal articular face. Dense hatching swatch (**A**) represents overlaid glue. The extent of the distal transverse breadth of Mt-I only appears longer in **F** compared to **B** because the metatarsal is ‘twisted’ about its long axis, as represented in **B**. Scale bar equals 10 cm.

extends distally to a rugose protuberance that forms part of medial condyle. The shaft proximal to the medial condyle expands, flaring dorsoplantarly, to form a symmetrical condyle in medial aspect (Fig. 9D). The lateral distal condyle is not as expanded as its medial counterpart, but is more rugose. The intercondylar groove is shallow and best expressed plantarily. Similar to Mt-II, a short distally positioned crest arises from the lateral condyle, whereas a short deep notch indents the adjacent lateral surface (Fig. 9G). The corresponding medial surface also houses a depression, though much shallower. On the plantar surface, a small fossa occupies the space proximal to the intercondylar groove. Further proximally, a low tubercle originates mid-shaft and extends to the proximal edge, where it is more prominent and rugose (Fig. 9B).

Metatarsal IV—Metatarsal IV (Fig. 10) has a more rounded shaft in its distal half than the preceding metatarsi. The distal end culminates in a moderately expanded distal articular surface. In contrast, the proximal half of Mt-IV is flattened and flared lateromedially. More so, the proximal end is less expanded, dorsoplantarly, than the shaft itself. Regarding the proximal surface, the plantar margin is proximally higher than the dorsal edge. The proximal surface rolls medially to grade into the shaft, but the opposite lateroproximal corner is faintly apical. The lateroproximal corner is especially narrow, but expands moderately laterally, resulting in a wedge-shaped proximal articular surface. The proximal half of the plantar surface is slightly depressed, but overall the plantar face is flatter but more pitted than the dorsal. Like metatarsi II–III, the medial condyle is larger than the lateral, which is partly due to the cylindrical shaft form. Although, the lateral corner is abraded, a short crest is present proximal to the articular surface. The intercondylar groove is best developed on the plantar side.

Non-terminal Phalanx of Digit I—Phalanx I-1 is segregated into two parts: the larger of these is a free unit comprising the proximal half and distal medial condyle (Fig. 11B–F); the distal lateral condyle fragment is adherent to the ungual (Fig. 11G–J). Viewed dorsally, phalanx I-1 (Fig. 11A–F) is rectangular, and lateromedially longer than it is proximodistally. The dorsal face

is moderately depressed, resulting in a distinct perimeter formed of proximal, lateral, and medial crests outlining the depression (Fig. 11C). A similar excavation is repeated on the plantar surface (Fig. 11D), where it is deeper but mainly bounded by a shelf-like eminence along the proximal edge. Proximally, phalanx I-1 is wedge-like, narrowing towards the lateral edge. The wedge profile results in the medial condyle being much larger than the lateral one (Fig. 11B, E). The lateral face is marked by a short median ridge, which extends from the proximal articular surface to articulate distally with the lateral condyle. Both condylar surfaces are arched, and face plantarily. On the lateral condyle, this is expressed as an abrupt plantar eminence (Fig. 11B, D). In contrast, the medial face is simple. The intercondylar groove is as deep as it is dorsoplantarly narrow. The proximal articular surface is flat except for a slight flaring along the plantar edge (Fig. 11D).

Non-terminal Phalanges of Digit II—The first phalanx of the second digit, II-1, is comparable to phalanx I-1 in size and morphology. It differs in having a larger proximal surface area (Fig. 12E), due mainly to an oval profile, though is similarly narrower laterally. The shortened shaft region of II-1 is not as constricted as the corresponding region in I-1, although the plantar surface is similarly excavated. Phalanx II-1 bears a symmetrical rounded condyle in medial view. The plantar area of the lateral condyle is as expanded as its medial counterpart but dorsally it is unexpanded, effectively forming an extension of the shaft. Similar to I-1, the plantar portion of the lateral condyle extends proximally. Additionally, in phalanx II-1, the lateral condyle flares laterally to form a prominent crest that joins the proximal surface. The dorsal part of this crest is sculptured before recessing into a deep ligament fovea. The unobscured margins of the distal region indicate that the intercondylar groove is expressed more strongly plantarly than dorsally. II-1 is the largest of the non-ungual pedal phalanges.

The second phalanx (Fig. 12A–D, G) is a trigonal element, comprised chiefly of well-developed condylar, or other, articular surfaces. Also, what little non-condylar bone that exists is slightly depressed, forming fossae both dorsally and plantarly on the element. The medial face of II-2 is simple, whereas the lateral region

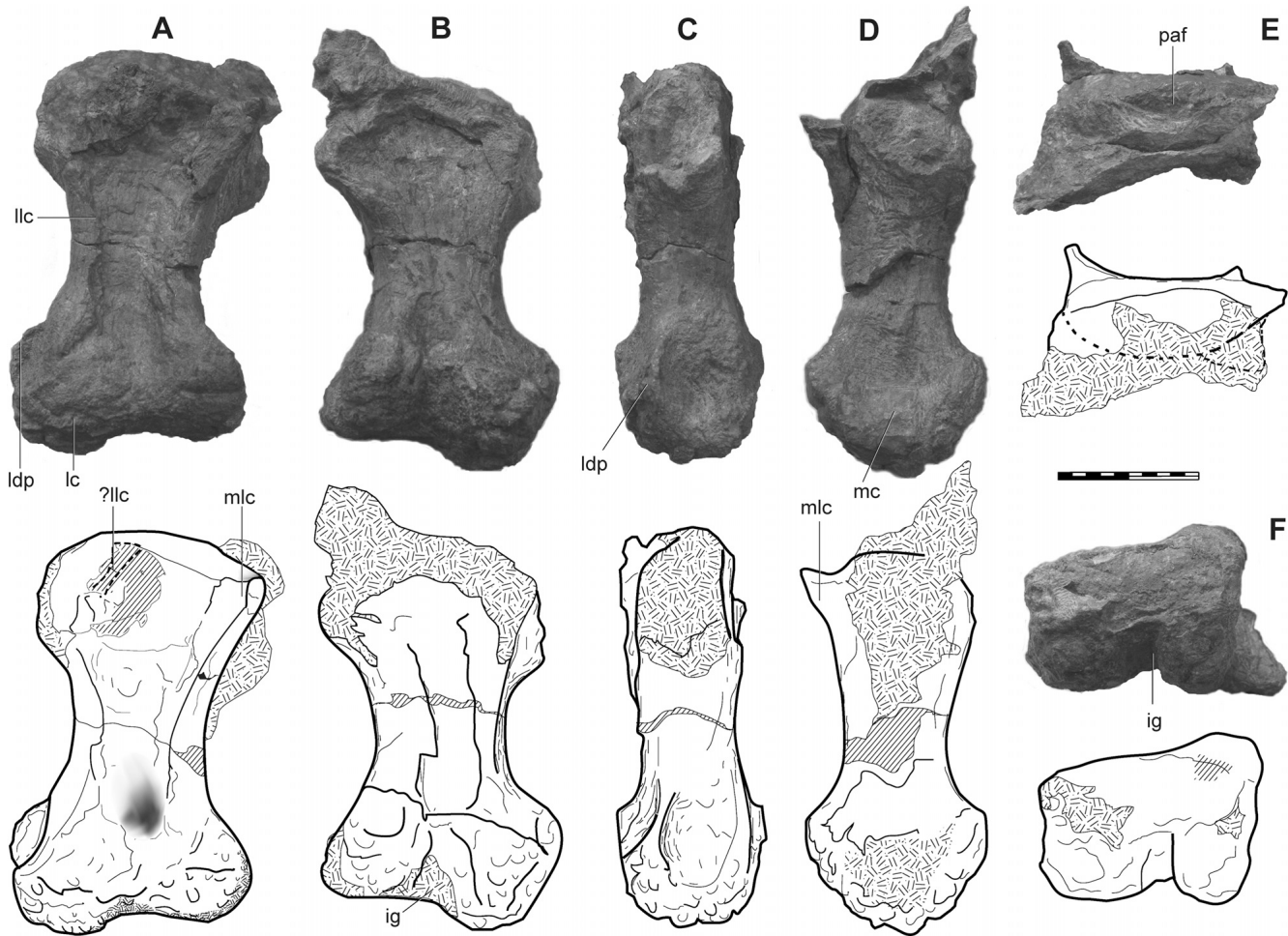


FIGURE 8. Metatarsal II of *Rhoetosaurus brownei*. **A**, dorsal; **B**, plantar; **C**, lateral; **D**, medial; **E**, proximal; **F**, distal views. Abbreviations: **ig**, intercondylar groove; **lc**, lateral condyle; **ldp**, laterodistal process; **llc**, lateral longitudinal crest; **mc**, medial condyle; **mlc**, medial longitudinal crest; **paf**, proximal articular face. Scale bar equals 10 cm.

is minimized to an apex, which unites the proximal and distal surfaces. A shallow intercondylar groove parts the lateral condyle from an asymmetrically shaped, plantarily expanded, medial condyle. Thus, the distal articular face resembles the analogous surface of the phalanx I-1, which also adjoins an ungual. However, unlike I-1, in II-2 the distal surface area is much less than the mostly obscured proximal area. The form of the proximal surface in II-2 can be inferred from the curved proximal edges in both dorsal and plantar views. Most likely, the proximal face is convex, and slopes distally toward the medial and lateral margins.

Non-terminal Phalanges of Digit III—Three non-terminal phalanges occur in digit III (Fig. 13). The most proximal of these, III-1, is more than twice as voluminous as the remaining two, III-2 and III-3, combined. The medial face of III-1 is less expanded than the lateral side, extending distally to about 70% of the same length of the lateral surface. The discrepancy is accounted for by positioning III-2, a relatively miniaturized element, between the medial condyle of III-1 and the medial half of the proximal articular facet of III-3. The distal region of III-1 has a well-formed condylar structure, whereas III-2 and III-3 represent elements of relatively undifferentiated morphology.

The proximal surface of III-1 is lenticular about a lateromedially longer axis (Fig. 13A). A shallow trough extending along the center of the proximal face is flanked by gently upturned

dorsal and plantar margins. In turn, the dorsal face of III-1 is rounded to reflect the proximal outline. On the plantar surface, the proximal margin forms a rugose rim overhanging a rectangular concavity that is bracketed by noticeably delineated margins (Fig. 13C). The bone texture in the concavity is further demarcated from the surrounding texture of the margins and condyles by its smoother surface texture. The medial border of the concavity is a short broad ridge that also outlines a shallow sulcus on the medial face of III-1. Though partly obscured by III-2 and matrix, the medial condyle of III-1 is approximately quadrangular. The lateral condyle, in contrast, is plantarily expanded (Fig. 13E). Beginning plantarily it curves dorsally obtusely to contact with III-2 before terminating acutely. The intercondylar groove is shallow, but furrows deeply plantarily, parting the rugose condyles, before opening into the fossa on the plantar face. A nutrient foramen is situated proximal to where the intercondylar groove extends onto the plantar face.

The rudimentary phalanx III-2 is a globular element that narrows laterally (Fig. 13C, F). Dorsally, it occupies a position distal to the medial condyle of III-1. In plantar view, it extends further laterally than the medial condyle of III-1 such that its rounded lateral apex adjoins part of the lateral condyle of III-1. Medially, the bone texture is trabeculate, indicating that outer lamellar bone has been lost.

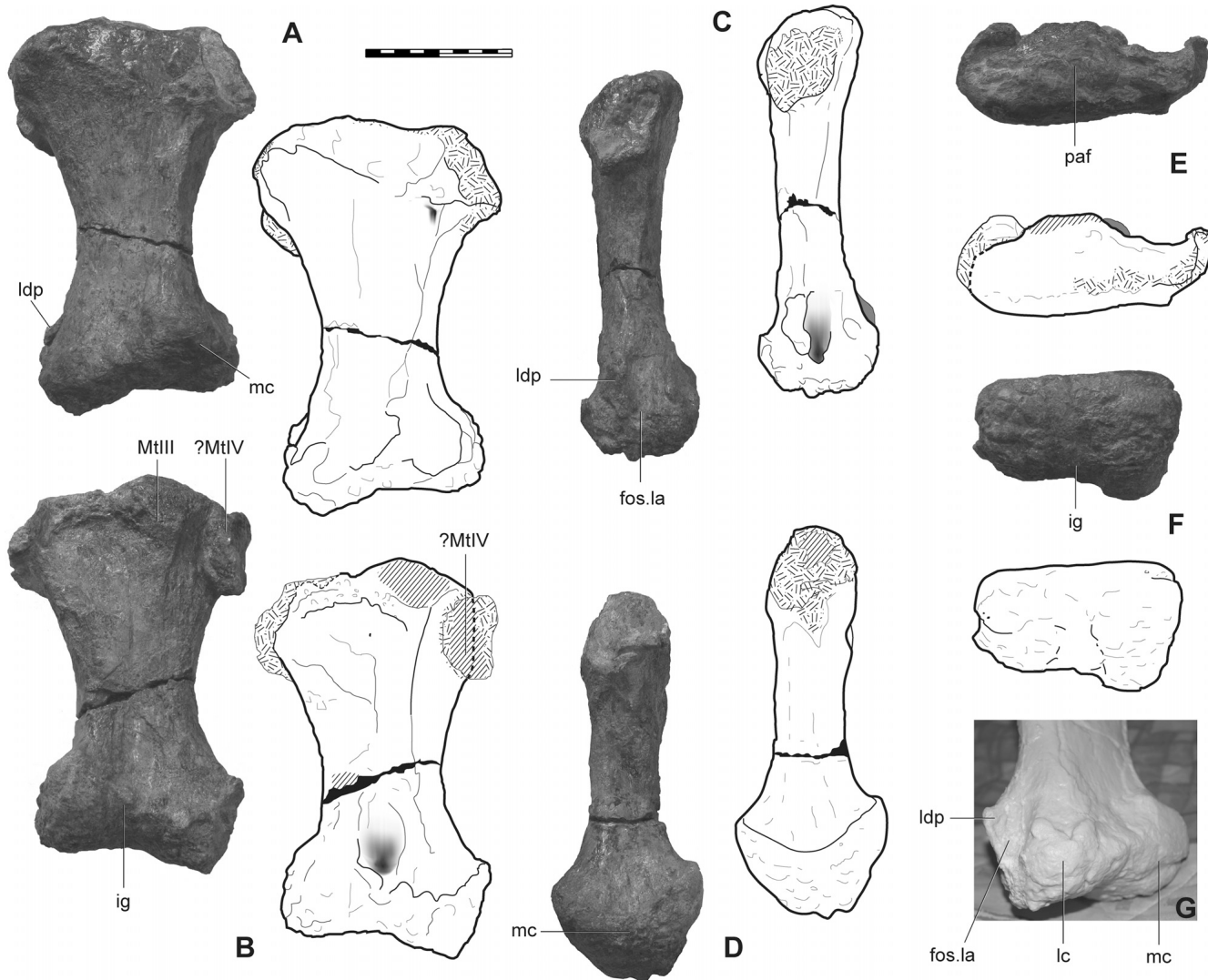


FIGURE 9. Metatarsal III of *Rhoetosaurus brownii*. **A**, dorsal; **B**, plantar; **C**, lateral; **D**, medial; **E**, proximal; **F**, distal views; **G**, distal end in laterodistal oblique view. Abbreviations: **fos.la**, laterodistal fossa; **ig**, intercondylar groove; **lc**, lateral condyle; **ldp**, laterodistal process; **mc**, medial condyle; **Mt IV**, fragment of metatarsal IV; **paf**, proximal articular face. Scale bar equals 10 cm.

Phalanx III-3 (Fig. 13B–F) is a proximodistally compressed bone. Although the lateral portion is too poorly preserved for detailed assessment, III-3 appears to narrow dorsoplantarly but concurrently expand proximodistally toward the lateral side. The medial view demonstrates a semi-lunate profile, with the flat side corresponding to the proximal margin. The plantar surface comprises trabeculate bone texture.

Non-terminal Phalanges of Digit IV—Phalanx IV-1 (Fig. 14A–F) bears a lenticular proximal face, not dissimilar to that of III-1. In contrast to III-1, the dorsoplantar breath of IV-1 is much smaller. Other similar traits to III-1 involve a lateral condyle extending further distally than the medial, a proximoplantar rugose rim, and a comparable fossa on the plantar face. Laterally, the bone linking the proximal face and distal lateral condyle is developed into a narrow rounded keel. The medial condyle is slightly more expanded than the lateral.

Phalanx IV-2 is too poorly preserved for detailed descriptive comments (Fig. 14A, C–F). It appears to be an elliptical to globular fragment. The dorsodistal exposure is trabeculate. The form of the bordering distal surface of IV-1 suggests that the medial

portion of IV-2 is probably proximodistally larger than the lateral one, though this region in IV-2 is mostly obscured.

General Comments on Unguals—All known terminal phalanges in *Rhoetosaurus* are mediolaterally compressed unguals, unlike the nubbin-like terminal phalanges seen in some sauropod pedes. On the proximal face of each ungual, an extensor tubercle is situated on the mediodorsal edge, whereas a flexor tubercle is located along the lateral edge (e.g., Fig. 12H). If the extensor and flexor tubercles are maintained in a subvertical plane in order to impart extension/flexion movement in a similar direction, then the unguals must be partially rotated laterally about their long axes (laterally) to accomplish this.

The proximal articular facets of the unguals are beveled, which contributes to the angled articulation between the claws and adjoining non-ungual phalanges (Bonnan, 2005). Specifically within the articular region of each ungual, the medio-proximal component extends further proximally than the latero-proximal counterpart. Consequently, this beveled articulation, in combination with some long-axial rotation, directs the claws laterally.

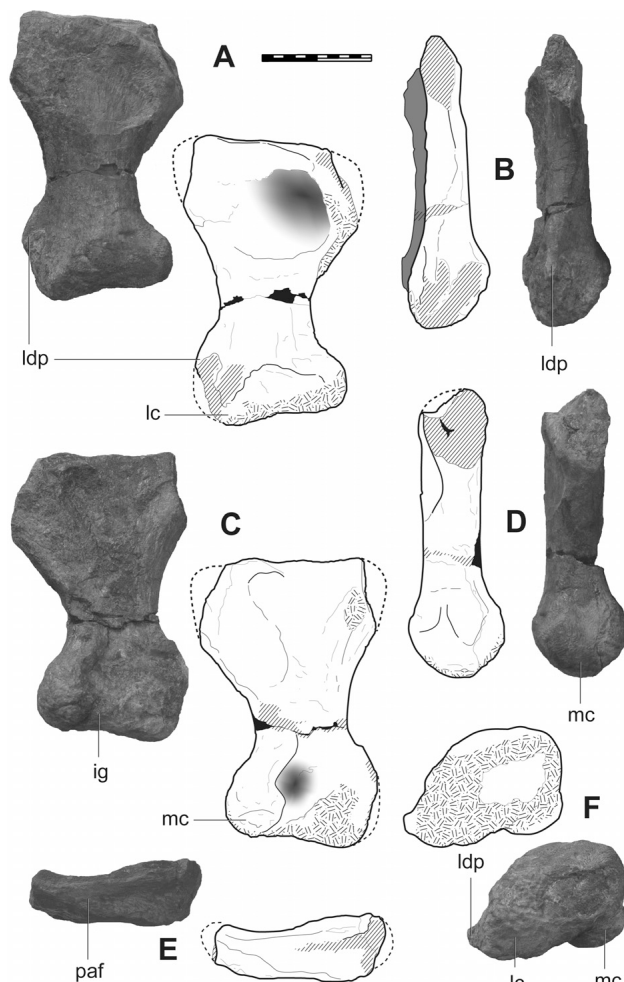


FIGURE 10. Metatarsal IV of *Rhoetosaurus brownei*. **A**, dorsal; **B**, lateral; **C**, plantar; **D**, medial; **E**, proximal; **F**, distal views. Abbreviations: **ig**, intercondylar groove; **lc**, lateral condyle; **ldp**, laterodistal process; **mc**, medial condyle; **paf**, proximal articular face. Scale bar equals 10 cm.

The unguals curve slightly plantomedially, but as they sequentially decrease in size they become less trenchant, partly due to the increased bluntness of the tips. An encasing claw sheath, as indicated by extensive claw grooves and other accessory nutrient pits, likely supported each claw when the animal was alive.

Ungual of Digit I—The second phalanx (I-2) of the hallux (Fig. 11G–L) is the most massive (as long as the largest metatarsi) and the most morphologically complex among the phalanges. The element is lateromedially compressed and deep dorsoventrally (the lateroventral face probably forms the plantar surface). Excluding the terminal 30% of the element, the near-parallel profiles of the dorsal and ventral margins maintain the deep appearance of the bone. The mid-region of the lateral face is indented, so that the terminal and proximal portions are lateromedially thicker than the mid-diaphysis.

The proximal articular face has a ‘U’-shaped outline, comprising a thick annulus bounding an indentation that received the lateral condyle of phalanx I-1 (Fig. 11K). Viewed proximally, this rim arcs around the plantar-most point, where it is thickest and also coincides with the flexor tubercle. The medial surface extends further proximally than the lateral counterpart, rendering the articular outline beveled with respect to the adjoining proximal phalanx. The extensor tubercle is represented by a protrusion

at the junction of proximal face and the mediadorsal margin (Fig. 11H). Additionally, the tubercle slightly overhangs above the proximal articular sulcus. The flexor tubercle is rugose and protuberant towards the lateroplantar side of the bone as a tuberosity. The bone has a collar-like constriction on the medioventral surface adjoining the tubercle (Fig. 11I). The flexor tubercle continues along the lateral face dorsally as an extension of proximal articular annulus.

The semi-oval outline of the proximal face opens dorsolaterally into a shallow sulcus, distinct from the proximal articulation. This sulcus is ‘V’-shaped, diverging proximally, towards the flexor and extensor tubercles (Fig. 11H, K). Toward the tip of the ungual, the sulcus narrows behind a protuberance, tapering into a nutrient groove (*sensu* ‘claw groove’) that extends parallel and close to the dorsal edge on the lateral surface of the bone (Fig. 11J, K). The groove is deepest near the lateral depression in the mid-claw region before petering out before it reaches the tip.

On the medial surface, a linear groove originates from the proximal annulus, about mid-point between the extensor and flexor tubercles. The groove extends obliquely across the medial face, adjacent to a fracture in the phalanx, and peters out before reaching the dorsal edge of the claw. The sculptured tip bears numerous vascular markings (Fig. 11L). The medial surface proximal to the tip is scoured by a dendritic furrow, which appears to be directed apically towards the tip. Numerous pits, some of which are up to 1 cm in diameter, puncture the lateral and plantar surfaces around the tip. The exterior texture around the medial side of the tip is covered by much smaller groove and pit markings.

Ungual of Digit II—The unguals of digits II and III retain the general traits of the hallux ungual, but sequentially differ subtly in shape. Accounting for its smaller size, ungual II-3 (Fig. 12G–L) is less lateromedially compressed along its dorsal margin than the hallux ungual, I-2. In contrast, it is ventrally narrower. In II-3, the caudal collar-like constriction near the proximal articular facet is further developed, augmenting the flexor tubercle. The lateroproximal margin is linear, and relatively longer in II-3 (than I-2), effectively broadening the extensor tubercle. Laterally, the surface of II-3 does not exhibit the sunken form seen in the mid-region of I-2. The claw groove, too, is shallower. The oblique groove, noted on the medial aspect of I-2, is now modified into a linear tuberosity that bounds the distal part of a shallow excavation in II-3 (Fig. 12I). The tip of the ungual in digit II is comparatively more rounded and contains fewer pits. Of all unguals, II-3 exhibits the greatest amount of curvature of the tip plantarily.

Ungual of Digit III—The noted differences between the hallux ungual, 1–2, and II-3 are further pronounced between it and the fourth ungual, III-4 (Fig. 13G–L). In III-4, the extensor tubercle is well developed in the form of an apical corner on a shelf-like extension of medial surface, which extends further proximally than its lateral counterpart. The flexor tubercle is the rim-like along the proximolateral margin. In lateral view, the articular sulcus extends further dorsally to lead into a barely noticeable and shallow nutrient groove. The dorsolateral surface near the tip is modified from the narrow edge seen in the preceding larger unguals to a flattened surface in III-4 (Fig. 13L). The oblique ridge and broad dorsal depression seen in II-3 (Fig. 12I) is transformed into a rounded fossa, with a less prominently bounding ridge in III-4 (Fig. 13I). A medial accessory groove, originating close to the flexor tubercle extends parallel to the proximoterminal axis to the tip (Fig. 13K).

Ungual of Digit IV—Phalanx IV-3 is a flattened bone that superficially appears less recurved than the preceding unguals, but this is likely due to abrasion of the terminal area. IV-3 differs from the larger unguals when aligned vertically along the long axis in several aspects. IV-3 curves dorsally and laterally along its longest axis, whereas the other unguals curve ventrally and

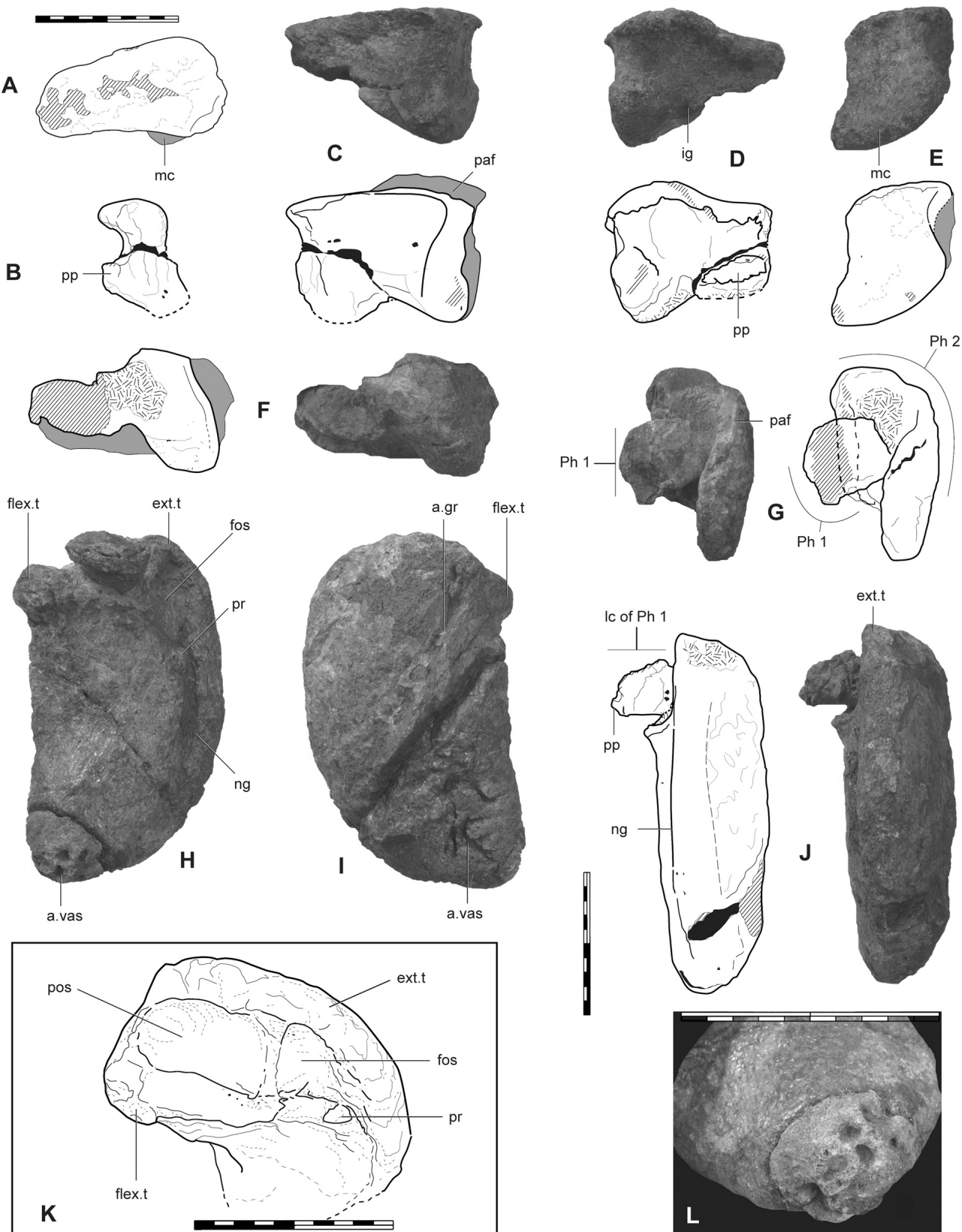


FIGURE 11. Phalanges of pedal digit I of *Rhoetosaurus brownei*. Non-terminal phalanx I-1 (**A–F**) in **A**, proximal; **B**, lateral; **C**, dorsal; **D**, plantar; **E**, medial; **F**, distal views. Ungual I-2 and adherent lateral condyle of non-terminal phalanx I-1 (**G–J**) in **G**, proximal; **H**, lateral; **I**, medial; **J**, dorsal views. Close ups of ungual (**K–L**) showing **K**, reconstructed proximolateral face without adherent non-terminal phalanx (based on a cast); **L**, terminal area highlighting external vascular structures (lateral side is above). **Abbreviations:** **a.vas**, accessory pits and vascular grooves; **a.gr**, accessory groove; **ext.t**, extensor tubercle; **flex.t**, flexor tubercle; **fos**, sulcus; **ig**, intercondylar groove; **lc**, lateral condyle; **mc**, medial condyle; **ng**, nutrient groove; **paf**, proximal articular facet; **Ph**, phalanx; **pos**, proximal articular sulcus; **pp**, plantar process; **pr**, protuberance. The interpretative drawings for **B–D** are based on reconstructed casts of the fragments comprising phalanx I-1. Scale bar equals 10 cm.

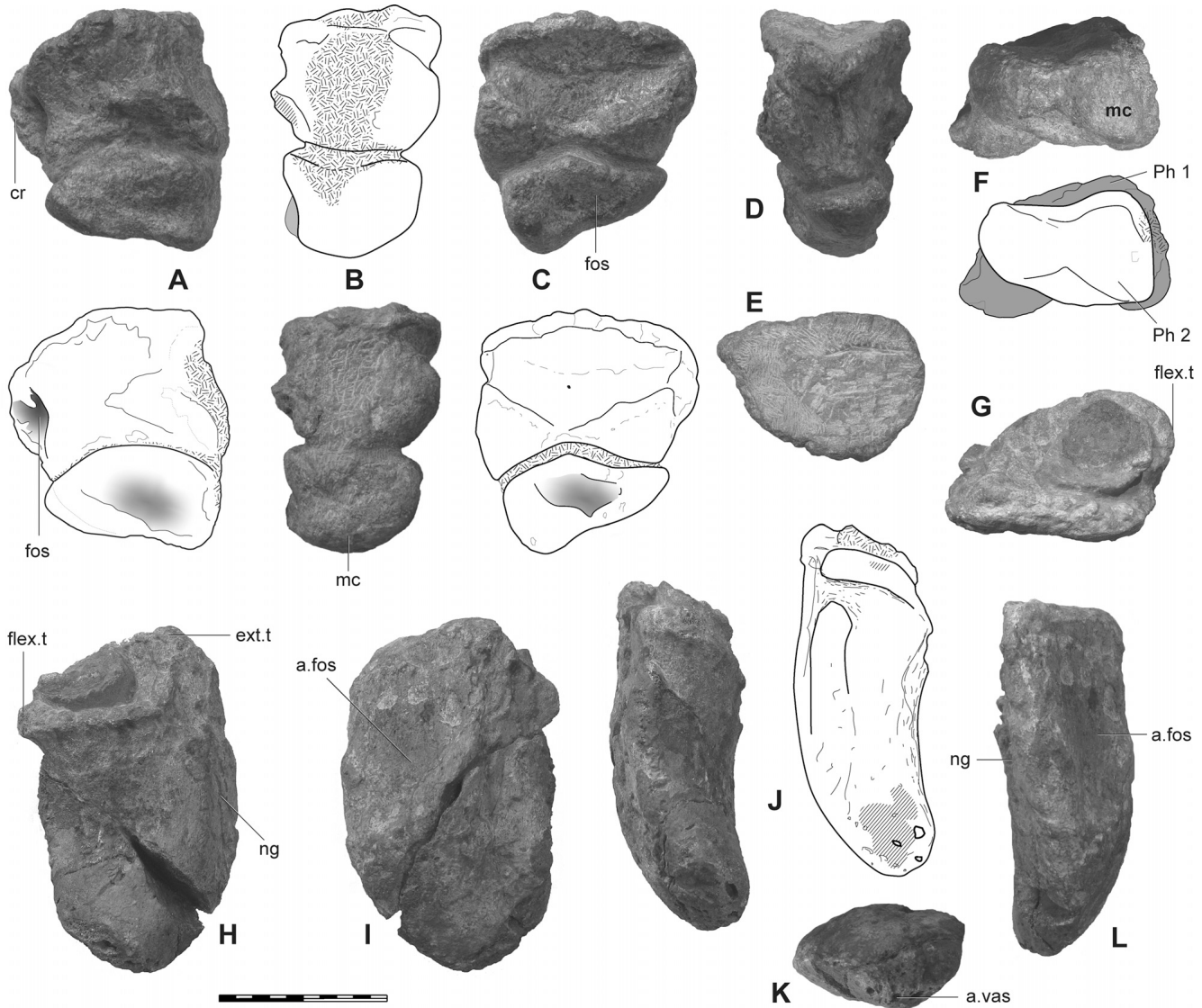


FIGURE 12. Phalanges of pedal digit II of *Rhoetosaurus brownei*. Non-terminal phalanges II-1 and II-2 (**A–F**) in **A**, dorsal; **B**, medial; **C**, plantar; **D**, lateral; **E**, proximal views. Ungual II-3 (**G–L**) in **G**, proximal; **H**, plantar; **I**, dorsal; **J**, medial; **K**, terminal; **L**, lateral views. **Abbreviations:** **a.vas**, accessory pits and vascular grooves; **a.fos**, accessory fossa; **ext.t**, extensor tubercle; **foss**, fossa; **flex.t**, flexor tubercle; **mc**, medial condyle; **ng**, nutrient groove; **Ph**, phalanx. Scale bar equals 10 cm.

laterally, respectively. In IV-3, the ventral margin forms the greater arc whereas the dorsal edge corresponds to the lesser circumference. Furthermore, whereas the proximal articular faces of the other unguals are oblique to the dorsoventral plane of each element, in IV-3 it is aligned close to this plane (Fig. 14G–I).

The proximal articulation is simple in IV-3, forming an elliptical indentation. The flexor tubercle is a minor protuberance. Except for the proximomedial edge of the ungual, no obvious candidate for an extensor tubercle is visible. Terminal to the proximal end the body is featureless. The surface texture, where it is not obscured by matrix, is either trabeculate (incomplete) or relatively smooth compared to the other unguals.

The opposing curvature and deviation in form at the proximal end of IV-3 with respect to the other larger unguals may support it being a phalanx of the left pes instead of the right. Yet no definitive left pedal elements have been recovered and the close association between IV-3 and other right pedal elements

warrants maintaining that IV-3, though aberrant in morphology, is a bone of the right pes.

Comparative Morphology

The hind limb osteology of *Rhoetosaurus* was compared with basal sauropods (~Late Triassic–Early Jurassic), basal gravisaursians (~Early Jurassic–Late Jurassic), and several neosauropods (see Table 1S in Supplementary Data).

Tibiae—As in all other sauropods, the tibial shaft of *Rhoetosaurus* is twisted about its long axis (Harris, 2006:supplementary information). *Melanorosaurus* (Galton et al., 2005), and basal sauropods, including *Blikanasaurus* (Galton and Van Heerden, 1998), *Lessemsaurus* (Pol and Powell, 2007), and *Kotasaurus* (Yadagiri, 2001), typically have more stoutly constructed tibiae than *Rhoetosaurus*, partly due to the tibiae of these early sauropods being shorter relative to their femora. Accordingly,

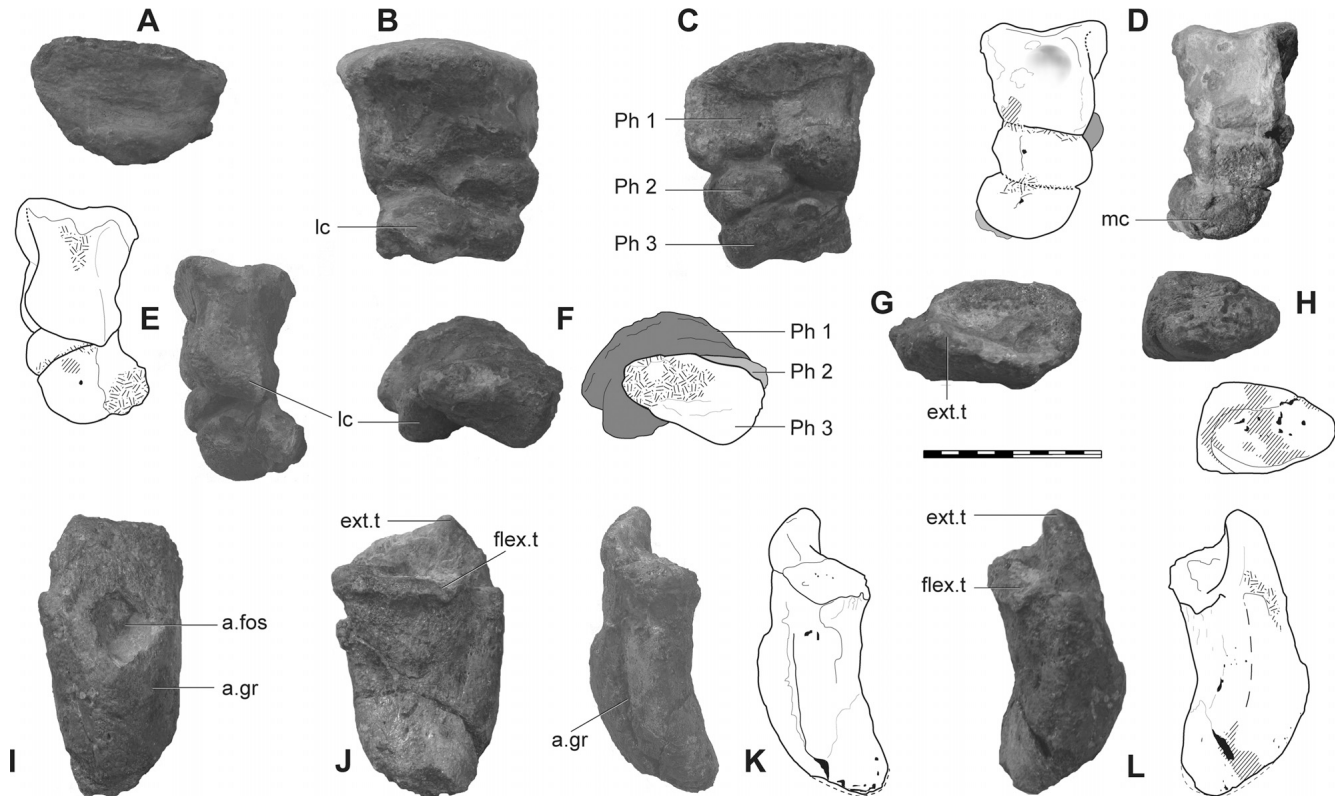


FIGURE 13. Phalanges of pedal digit III of *Rhoetosaurus brownei*. Non-terminal phalanges III-1, III-2, and III-3 (A–F) in A, proximal; B, dorsal; C, plantar; D, medial; E, lateral; F, distal views. Ungual of pedal digit IV (G–L) in G, proximal; H, terminal; I, dorsal; J, plantar; K, medial; L, lateral views. Abbreviations: a.fos, accessory fossa; a.gr, accessory groove; ext.t, extensor tubercle; flex.t, flexor tubercle; lc, lateral condyle; mc, medial condyle; Ph, phalanx. Scale bar equals 10 cm.

the cnemial crest in these basal genera is relatively more extensive than in *Rhoetosaurus*, occupying a third or more of the tibial length. Proximally, the rounded cnemial crest outline of *Rhoetosaurus* is reminiscent of that of *Ohmdenosaurus* (Wild, 1978), which appears also to be the earliest sauropod to have a comparatively gracile tibia similar to *Rhoetosaurus*, unlike the robust tibiae of other early sauropods. A feature separating *Rhoetosaurus* from the aforementioned sauropods is the greater development of the lateromedial breadth at the distal extremity in *Rhoetosaurus*, which is also present in more-derived sauropods. Tibiae of *Vulcanodon* (Cooper, 1984), *Shunosaurus* (Zhang, 1988), and neosauropods become increasingly more expanded distally, compared to the proximal region. *Rhoetosaurus* bears similarities to *Ferganasaurus* (Alifanov and Averianov, 2003) and more-derived sauropods, such as having similar fibula/tibia length ratios (around 105%), and a shortened cnemial crest compared to most Late Triassic sauropods. However, the straight, tabular cnemial crest of *Rhoetosaurus* differs from the rounded and more laterally flared structure observed in the diplodocoids, including *Apatosaurus* spp. (Gilmore, 1936; Upchurch et al., 2004b), *Barosaurus* (McIntosh, 2005), *Suuwassea* (Harris, 2007), *Tornieria* (Janensch, 1961), and macronarians, including *Camarasaurus* (Ostrom and McIntosh, 1966), *Brachiosaurus* (Janensch, 1961), and *Gobititan* (You et al., 2003). The cnemial crest in *Spinophorosaurus* (Remes et al., 2009), *Omeisaurus tianfuensis* (He et al., 1988), *Mamenchisaurus hochuanensis* (Young and Zhao, 1972), and *Patagosaurus* (Bonaparte, 1986) differ from that of *Rhoetosaurus*, being larger fan-shaped structures that are orientated predominantly cranially (craniolaterally in

Spinophorosaurus), instead of laterally. *Janenschia* (Bonaparte et al., 2000), however, possesses a trapezoid cnemial crest as in *Rhoetosaurus*. Although partly obscured by the fibula, *Rhoetosaurus* lacks the proximodistally trending elongate fossa on the caudal surface of the tibia that appears distinctive of both *O. tianfuensis* and *M. hochuanensis* (Tang et al., 2001).

The tibia of *Rhoetosaurus* differs from tibiae of all other sauropods in the expression of crests and sulci on the distal part of the medial surface. A crenulated surface in this region is depicted for *Camarasaurus* (Ostrom and McIntosh, 1966:213–215), but the area simultaneously lacks the very distinct combination of crests and sulci noted in *Rhoetosaurus*. Other sauropods probably contained similar, if less prominent, soft-tissue scars on the medial tibial surface, but it appears that such features may have been under-documented in the literature for sauropods in general. The medial crests and furrows, to the extent that they are developed in *Rhoetosaurus*, are unknown for any other sauropod. Similarly, the concentric proximal fossa present on medial surface of tibia is aberrant amongst sauropods. It resembles similar structures on proximal extremity of the fibula of *Opisthocoelicaudia* that were labeled foveae ligamentosa and assumed to be insertion points of pelvic-limb musculature (Borsuk-Bialynicka, 1977:40).

Fibulae—The fibula/tibia length ratio in *Rhoetosaurus* exceeded 1, a condition observed in all other sauropods, which resulted in the fibula gaining propinquity to the outer metatarsi. The craniocaudally elongate proximal outline is typical for most sauropods, though it is rectangular in *Rhoetosaurus* compared to the generally ovate outline in other taxa. It is possible the shape of the proximal fibula could be additionally accentuated by

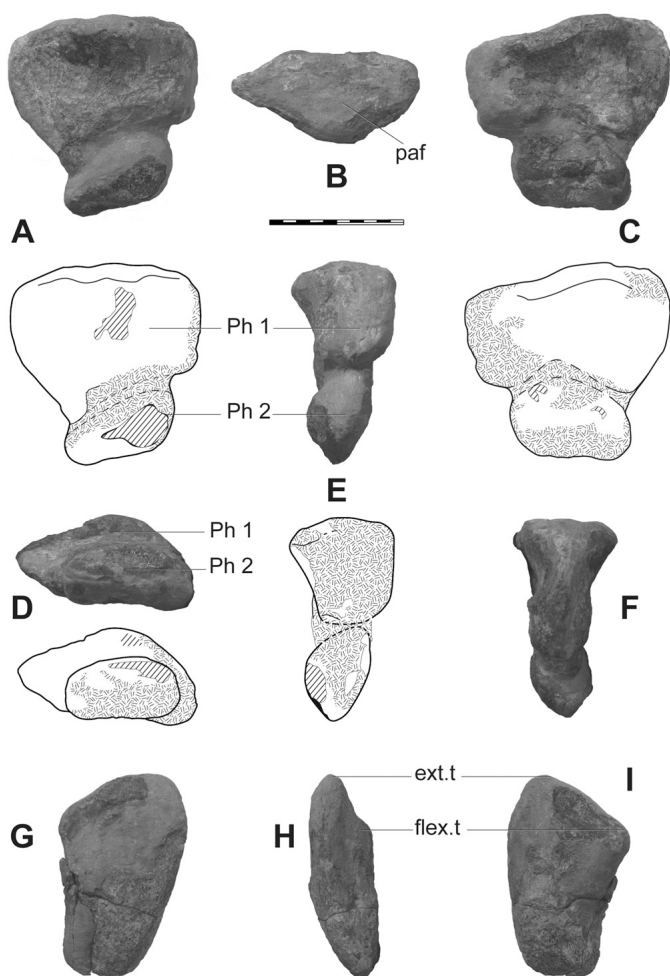


FIGURE 14. Phalanges of pedal digit IV of *Rhoetosaurus brownrei*. Non-terminal phalanges IV-1 and IV-2 (**A–F**) in **A**, dorsal; **B**, proximal; **C**, plantar; **D**, distal; **E**, medial; **F**, lateral views. Ungual of pedal digit IV in **G**, dorsal; **H**, medial; **I**, plantar views. Abbreviations: **ext.t**, extensor tubercle; **flex.t**, flexor tubercle; **paf**, proximal articular face; **Ph**, phalanx. Scale bar equals 10 cm.

preservational flattening. In *Rhoetosaurus*, the fibula is robust for its length, especially in the shaft, unlike the gracile fibulae seen in most diplodocoids (Hatcher, 1901; McIntosh, 2005; Harris, 2007) except *Apatosaurus* spp. (Gilmore, 1936; Upchurch et al., 2004b). The fibula shaft of many sauropods is flattened, whereas it is more rounded in *Rhoetosaurus*.

Most eusauropods bear a muscle scar or ridge usually midway along the lateral face of the fibula shaft, the tuberculum for the m. iliofibularis (Harris, 2007), which, in *Rhoetosaurus*, is not expressed strongly enough to allow its recognition. The tubercle for the m. iliofibularis occurs as a prominent longitudinal scar in *Ferganasaurus* and *Opisthocelicaudia*, whereas in *Camarasaurus* and *Limaysaurus* (Calvo and Salgado, 1995) it is as a depression, the m. iliofibularis sulcus (Harris, 2007) centered within an ovate rim. An arrangement of two elongate ridges and an intermediate sulcus is more strongly developed in *Suuwassea* than in other diplodocoids (Harris, 2007:17), demonstrating the variability of these features within subclades of sauropods. Nonetheless, the lack of any feature on the lateral surface of the fibula appears unique for this specimen among sauropods.

The distally positioned medial fossa in *Rhoetosaurus* is deeper and more extensive than in other sauropods except in *Janenschia*

(Janensch, 1961) and *Omeisaurus tianfuensis* (He et al., 1988). It is similar in outline but deeper compared to that in *Suuwassea* (Harris, 2007). Similarly, the corresponding lateral surface in *Rhoetosaurus* is more depressed than in other sauropods, partly on account of the greater mediolateral expansion of the distal extremity in *Rhoetosaurus*, particularly laterally. Amongst basal sauropods, the distal fibula face of *Kotasaurus* is more expanded mediolaterally than the proximal surface (Yadagiri, 2001), as also noted for *Rhoetosaurus*, whereas in *Blikanasaurus*, the distal extremity is similarly inclined distolaterally (Galton and Van Heerden, 1998).

Astragali—Comparing the astragalar morphology of *Rhoetosaurus* to other sauropods is difficult due to the state of preservation in QM F1659. Perhaps rare, the ‘exemplar b’ specimen of *Euhelopus* (Wilson and Upchurch, 2009) also includes an astragagus interlocked with the distal tibia. Regardless, the astragalar form of *Rhoetosaurus* is largely dissimilar in morphology to previously described sauropod exemplars. In *Melanorosaurus* and basal sauropods such as *Blikanasaurus*, *Lessemisaurus*, *Kotasaurus*, and *Omeisaurus tianfuensis*, the astragagus is quadrangular in outline when viewed distally, comprising a medial edge as long as the lateral one (He et al., 1988; Galton and Van Heerden, 1998; Yadagiri, 2001; Galton et al., 2005; Pol and Powell, 2007). In contrast, *Rhoetosaurus* shares with forms such as *Ohmdenosaurus*, *Vulcanodon*, *Ferganasaurus*, and neosauropods an astragagus that narrows medially in distal aspect, to form a medial projection. Among sauropods that have a medial process, the triangular form of it in *Rhoetosaurus* is distinguished from the rounded outlines found in diplodocoids, including *Apatosaurus ajax* (Upchurch et al., 2004b), *Diplodocus carnegii* (Hatcher, 1901), *Tornieria* (Remes, 2006), and *Dyslocosaurus* (McIntosh et al., 1992). In this regard, the profile of the medial process in *Rhoetosaurus* is similar to the more triangular outlines of *Vulcanodon*, *Ferganasaurus*, and *Epachthosaurus* (Martinez et al., 2004). The astragali of most eusauropods taper medially when observed cranially. This is only slightly developed in *Rhoetosaurus* and *Omeisaurus tianfuensis* (He et al., 1988), but is a more pronounced feature in titanosauriform macronarians (e.g., *Gobititan*, You et al., 2003). In these titanosauriform astragali, not only do the distal and proximal surfaces meet each other medially, but also the astragagus fails to cap the entire distal end of the tibia. However, the proximal astragalar area in *Rhoetosaurus* is equal to or greater than the distal tibial area, which is typically seen in non-titanosauriform sauropods.

The caudal astragalar sulcus in *Rhoetosaurus*, although poorly preserved, is simple unlike the more complex deep fossa incorporating foramina described for many sauropods (Fraas, 1908; Wilson and Sereno, 1998:29). The proximal astragalar surface in *Rhoetosaurus*, with its apparent lack of ascending process, is not comparable to other sauropods. The astragagus of the sauropod that most closely approaches the form in *Rhoetosaurus* is *Ohmdenosaurus* (where the ascending process forms a low bump; Wild, 1978). Finally, the presence of a distal roller is the norm for eusauropods. Although the distal astragalar surface is poorly preserved in *Rhoetosaurus*, the flat distal profile in *Rhoetosaurus* bears resemblance to the corresponding astragalar surface in *Ohmdenosaurus*, which additionally shares with *Rhoetosaurus* a very compressed proximodistal length.

Metatarsi—The metatarsus of *Rhoetosaurus* is atypical amongst sauropods. Each metatarsal, particularly within the proximal half, is compressed dorsoplantarly, which renders the proximal surfaces lateromedially elongate (Fig. 2A). The result, notably, is that the articulated metatarsal bridge (Figs. 2A, 15) is gracile compared to the corresponding structures of other sauropods (Fig. 15). The proximal outline of Mt-I of many other sauropods is dorsoplantarly longer and characteristically ‘D’-shaped, with the straight of the ‘D’ facing laterally. The proximal outline of Mt-II is generally rectangular, and followed by the

TABLE 1. Phalangeal and ungual formulas of sauropods compared.

Taxon	Phalanges	Unguals	References and comments
<i>Blikanasaurus cromptoni</i>	2-3-4-5-?1	1-1-1-?1-0	Galton and van Heerden (1998); digit IV is incomplete but the morphology of the last preserved phalanx suggests an additional terminal phalanx or phalanges.
<i>Gongxianosaurus shubeiensis</i>	2-3-4-5-?	1-1-1-1-?	He et al. (1998).
<i>Vulcanodon karibaensis</i>	2-3-4-?-?	1-1-1-?-?	Raath (1972).
<i>Rhoetosaurus brownii</i>	2-3-4-3-?	1-1-1-1-?	This study.
<i>Shunosaurus lii</i>	2-3-3-3-2	1-1-1-1-0	Zhang (1988:61, pl. 17).
FMNH 241-50 ('Pleurocoelus sp.')	2-3-4-2-0	1-1-1-1-0	FMNH 241-50 (Gallup, 1989) is purported titanosauriform but appears to have phalangeal and ungual counts evocative of a basal eusauropod. It has likely been phylogenetically misidentified and/or its anatomy requires investigation.
<i>Omeisaurus maoianus</i>	2-3-3-3-?2	1-1-1-0-0	Tang et al. (2001).
<i>Omeisaurus tianfuensis</i>	2-3-3-3-2	1-1-1-0-0	He et al. (1988:68, pl. 17).
<i>Dyslocosaurus polyonychius</i>	2-?2-?3-?2-?1	1-1-1-?1-?1	The pes of <i>Dyslocosaurus</i> exhibits diplodocoid morphology but bears four, or five unguals. Issues of phalangeal association in this taxon have been noted (McIntosh et al., 1992; Wilson and Sereno, 1998).
<i>Apatosaurus</i> sp. CMNH 89	2-3-4-2-1	1-1-1-0-0	Hatcher (1901:54), Gilmore (1936), and Bonnan (2005). Although often referred to <i>Apatosaurus excelsus</i> , Upchurch et al. (2004b) could not assign it to any particular species taxon based on established autapomorphies of apatosaurine species. Digit III comprises four phalanges.
<i>Apatosaurus ajax</i>	2-3-3-2-1	1-1-1-0-0	Upchurch et al. (2004b).
<i>Apatosaurus louisae</i>	2-3-?3-2-?	1-1-1-0-0	Gilmore (1936:240) suggested digit III had four phalanges based on comparison to CMNH 89 (Gilmore, 1936:234); digit III preserves three phalanges.
<i>Barosaurus lentus</i> AMNH 6341	2-3-3-2-2	1-1-1-0-0	Gilmore (1932:20). McIntosh (2005) referred this specimen (previously assigned to <i>Diplodocus</i>) to <i>Barosaurus</i> .
<i>Barosaurus lentus</i> AMNH rotunda cast	2-3-2-2-1	1-1-?0-0-0	Rothschild and Molnar (2005:fig. 17.5). The AMNH rotunda display is a cast of AMNH 6341 (McIntosh, 2005), so the rationale for restoring only two unguals is not apparent.
<i>Diplodocus carnegii</i>	2-3-3-2-1	1-1-1-0-0	Bedell and Trexler (2005:308).
<i>Camarasaurus lentus</i> (USNM 13786)	2-3-3-2-1	1-1-1-0-0	McIntosh et al. (1996:24).
<i>Janenschia robusta</i>	2-3-3-2-1	1-1-1-?-0	Bonaparte et al. (2000:fig. 8) illustrated a very trenchant first ungual, but the tip of this is missing (Fraas, 1908:pl. 12) and has been restored (Janensch, 1961:pl. 23).
<i>Tangvayosaurus hoffeti</i>	2-3-3-2-1	1-1-1-0-0	Allain et al. (1999).
<i>Gobititan shenzhouensis</i>	2-2-2-2-2	1-1-1-0-0	You et al. (2003). The three unguals are sub-equal in length, which may be an autapomorphy for <i>Gobititan</i> .
<i>Epachthosaurus sciuttoi</i>	2-2-3-2-0	1-1-1-0-0	Martinez et al. (2004).
<i>Euhelopus zydzanskyi</i>	?2-?3-?1-?2-?	?1-0-?-?	The proximal phalanx of digit I is missing in the reconstruction provided by Wiman (1929:pl. 4); whereas the positioning of all purported unguals is in doubt based on morphology (Wilson and Upchurch, 2009).
MUCPv-1533 (unnamed form, from Neuquén)	2-2-2-2-0	1-1-1-0-0	Gonzalez-Riga et al. (2008).
<i>Opisthocoelicaudia skarzynskii</i>	2-2-2-?1-?	1-1-1-?-?	Wilson (2005:32).

Phalangeal formulas are conveyed in the notation of Padian (1992), where '0' indicates the metapodial is present but phalanges missing.

more variable proximal outlines of Mt-III–V, which range from triangular to lenticular shapes (Fig. 15). Whereas the proximal outlines of Mt-III or Mt-IV may be lateromedially longer than dorsoplantarly in some sauropods such as in *Cetiosauriscus* (Heathcote, 2002), *Omeisaurus maoianus* (Tang et al., 2001), or *Epachthosaurus* (Martinez et al., 2004), the surrounding metatarsi tend to be more dorsoplantarly expansive. Only in *Shunosaurus* (Zhang, 1988:fig. 55) do the mediolaterally elongate proximal outlines of all metatarsi approach the condition observed for *Rhoetosaurus*, although in *Rhoetosaurus* the proximal bridge is even further dorsoplantarly compressed.

The maximum length of the first metatarsal in *Rhoetosaurus* is 27% of the proximodistal length of the tibia, and thus similar to *Melanorosaurus* (26%, Galton et al., 2005) and *Antetonitrus* (24%, Yates and Kitching, 2003) but distinct from neosauropods (Fig. 16A) such as *Barosaurus* (13%, McIntosh, 2005) or *Epachthosaurus* (18%, Martinez et al., 2004). The longest metatarsal in most sauropods is the third, of which the Mt-III/tibia ratio gives an indication of the degree of shortening of the metatarsus overall (Fig. 16A; Yates and Kitching, 2003).

In *Rhoetosaurus*, Mt-III is 34% the tibial length, hence grouping with *Melanorosaurus* and the basal sauropods *Antetonitrus*, *Omeisaurus maoianus*, and *Vulcanodon* (45%, 38%, 38%, 37%, respectively; Fig. 16B). The same ratio is 25% and 27% in *Shunosaurus* and *Omeisaurus tianfuensis*, respectively (Tang et al., 2001:101), and between 18% and 25% for neosauropods.

The presence of a laterally emanating tabular extension of the lateral condyle in the first metatarsal has been considered a synapomorphy of Diplodocidae (McIntosh, 1990; Bonnan, 2005). Similar distolateral processes occur in metatarsi I–III of *Rhoetosaurus*, and have also been noted on Mt-I of *Shunosaurus* and *Omeisaurus* spp. (He et al., 1988; Upchurch, 1998; Tang et al., 2001). In Mt-I of *Rhoetosaurus*, the process does not flare laterally as much as in diplodocids (Fig. 17), but it is a prominent crest in metatarsi II–III, hence not dissimilar to the process on Mt-I of diplodocids. Further, the laterodistal process on Mt-I is a more widely distributed feature in non-macronarian sauropods (Fig. 17) than previously thought, occurring in non-diplodocids such as *Cetiosauriscus* (Heathcote, 2002), *Janenschia* (Fraas, 1908:pls. 11–12), and *Tastavinsaurus* (Canudo et al., 2008).

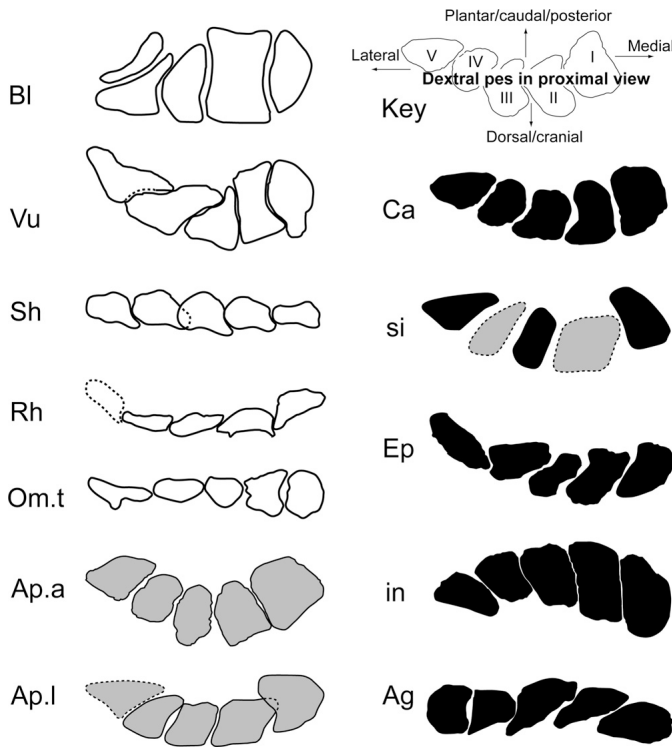


FIGURE 15. Line drawings comparing the metatarsal ‘bridge,’ in proximal view, of *Rhoetosaurus brownii* with that of other sauropods. **Taxic Abbreviations:** Ag, *Agustinia ligabuei*; Ap.a, *Apatosaurus ajax*; Ap.l, *Apatosaurus louisae*; Bl, *Blikanasaurus cromptoni*; Ca, *Camarasaurus gracilis*; Ep, *Epachthosaurus sciuttoi*; in, unnamed titanosaurian pes from La Invernada, Argentina; Om.t, *Omeisaurus tiansuensis*; Rh, *Rhoetosaurus brownii*; Sh, *Shunosaurus lii*; si, unnamed macronarian pes from Siberia; Vu, *Vulcanodon karibaensis*. Non-neosaurodops in clear, diplodocoids in grey, and macronarians in black tone. Sources of all drawings and notes on them are listed in Table 1S of Supplementary Data. Simstral-side elements are shown in reverse for ease of comparison. Not to scale.

Averianov et al. (2002) reported the feature in an unnamed titanosauriform from Siberia; however, this region of Mt-I is incomplete (Fig. 17A). The character is further present on metatarsi other than Mt-I (Fig. 17B), in *Cetiosauriscus*, *Omeisaurus* spp. (He et al., 1988; Tang et al., 2001), *Rhoetosaurus*, and the diplodocoids *Apatosaurus louisae* (Gilmore, 1936) and *Dyslocosaurus* (McIntosh et al., 1992).

The prominent ridges on the dorsal faces of metatarsi I–III, and especially those on Mt-II, of *Rhoetosaurus*, are also present less markedly in diplodocids (Bonnan, 2005). Overall, the metatarsus of *Rhoetosaurus* differs considerably from other sauropods by the dorsoplantarly compressed form proximally. In turn, this renders the distal halves of the metatarsi stout relative to the proximal ends, when the opposite is noted for other sauropods.

Phalanges—The phalangeal (and ungual) counts of *Rhoetosaurus* were compared to other sauropods (Table 1). *Rhoetosaurus* shares with sauropods more derived than *Blikanasaurus* and *Gongxianosaurus* a reduction from five to three or fewer phalanges in the fourth digit. However, based solely on phalangeal formula, it is differentiated from neosaurodops taxa, in which further loss of phalanges resulted in a count, typically, of 2-3-3-3-2, or fewer elements, with some variation having evidently occurred. *Rhoetosaurus* shares with *Vulcanodon* four phalanges in digit III. Gilmore (1936:240) considered four phalanges made up digit III in *Apatosaurus louisae* (but noted the “third pha-

lanx was missing”) based on comparative morphology with CM 89, *Apatosaurus* sp., which actually has an additional phalangeal ossification (diminutive) in digit III (Hatcher, 1901:52). Assuming Gilmore (1936) was mistaken regarding *Apatosaurus louisae*,

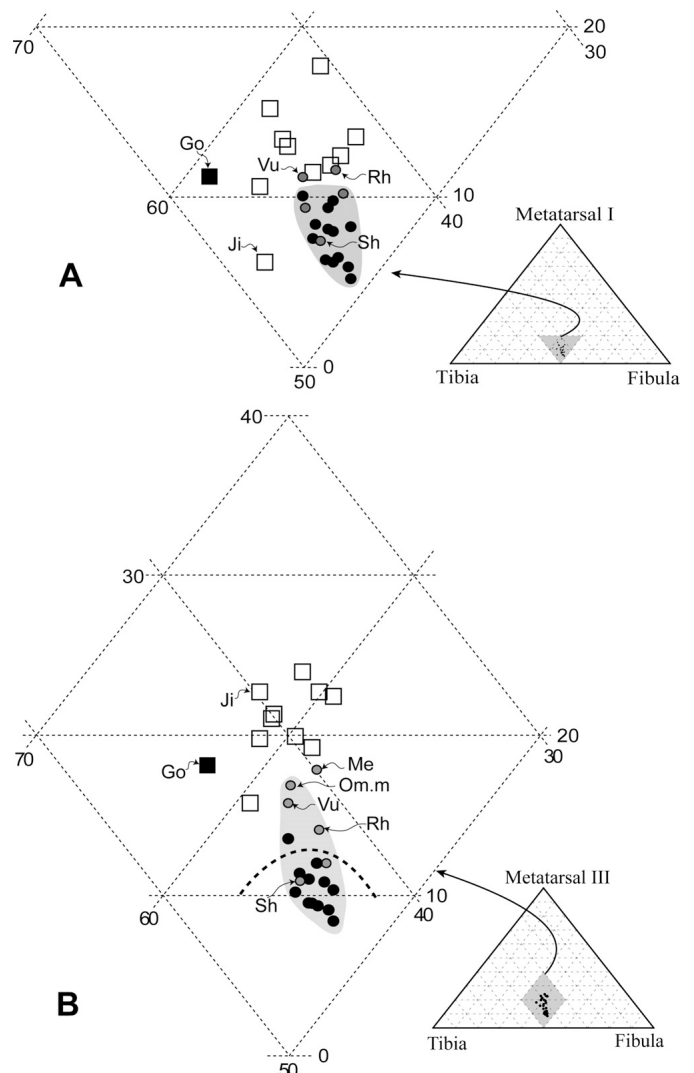


FIGURE 16. Trivariate distribution of crus (tibia, fibula) and metatarsal proportions in sauropodomorphs. Open squares are non-sauropod prosauropods; solid squares are potential early sauropods; grey dots are non-neosaurodops sauropods, and are mostly basal eusauropods; solid dots are neosaurodops. **A**, Mt-I and crus proportions: all sauropodomorph Mt-I lengths are within 0–20% the lengths of tibia or fibula, hence occupying a small zone within the ternary morphospace (expanded figure). *Rhoetosaurus* falls within a ‘transitional’ area between the two clusters of sauropodomorphs: (1) non-sauropod prosauropods, which usually have Mt-I exceeding 10% of tibial length, and (2) neosaurodops (grey tone), which all have a fibula longer than tibia and Mt-I less than 10% of tibial length. **B**, Mt-III and crus proportions: all sauropodomorph Mt-III lengths are within 5–25% the lengths of tibia or fibula, hence occupying a small zone within the ternary morphospace (expanded figure). *Rhoetosaurus* is positioned between neosaurodops and most non-neosaurodops, indicating its intermediate Mt-III/crus proportions. Grey tone indicates gravisaurian sauropods. The dashed line separates sauropods with a shortened pes (as indicated by Mt-III length) from those with a plesiomorphically longer pes. **Taxic Abbreviations:** Go, *Gongxianosaurus shibeiniensis*; Ji, *Jingshanosaurus xinwaensis*; Me, *Melanorosaurus readi*; Om.m, *Omeisaurus maoiansus*; Rh, *Rhoetosaurus brownii*; Sh, *Shunosaurus lii*; Vu, *Vulcanodon karibaensis*. Data sources are listed in Table 1S of Supplementary Data.

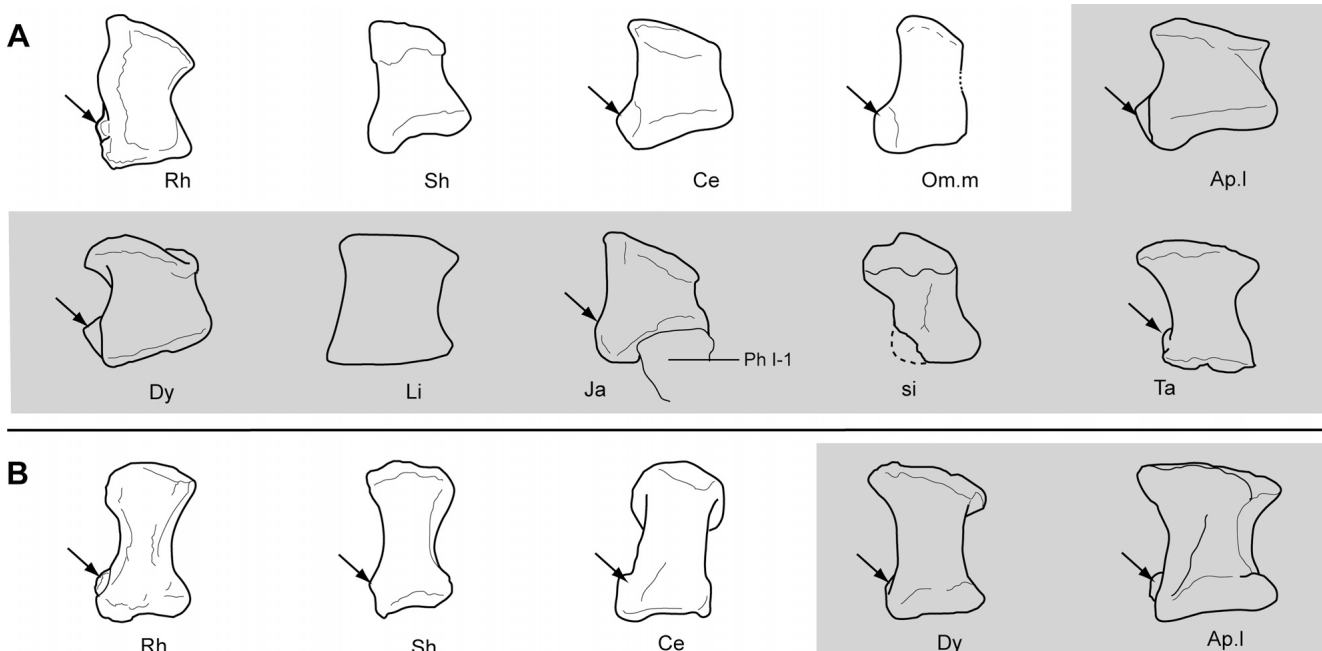


FIGURE 17. Line drawings comparing metatarsi of *Rhoetosaurus brownei* with those of other sauropods: **A**, first metatarsi; **B**, second metatarsi. **Taxic Abbreviations:** **Ap.I**, *Apatosaurus louisae*; **Ce**, *Cetiosauriscus stewarti*; **Dy**, *Dyslocosaurus polyonychius*; **Ja**, *Janenschia robusta*; **Li**, *Limaysaurus tessonei*; **Om.m**, *Omeisaurus maoianus*; **Rh**, *Rhoetosaurus brownei*; **Sh**, *Shunosaurus lii*; **si**, unnamed macronarian pes from Siberia; **Ta**, *Tastavinsaurus sanzi*. Neosauropods are shown in the shaded area. Sources of all drawings are listed in Table 1S of Supplementary Data. Drawings of sinistral-side elements are shown in reverse for ease of comparison. Arrows indicate laterodistal process (see text for discussion). All views are dorsal, and drawings not to scale.

all neosauropods have three or fewer phalanges making up digit III. *Rhoetosaurus* may be also be distinguished from some eusauropods by the same feature: only three phalanges are recorded in digit III of the eusauropods *Shunosaurus* and *Omeisaurus* spp. (Table 1). *Rhoetosaurus* bears four ungual terminal phalanges, distinguishing it from *Omeisaurus* spp. and neosauropods, which only contain three or fewer.

The unguals of *Rhoetosaurus* progressively decrease in size, as they do in all non-titanosauriform sauropods, whereas the first two unguals in *Epachthosaurus* (Martinez et al., 2004) and *Gobitan* (You et al., 2003) are equal in size. Similar to other sauropods, the unguals of *Rhoetosaurus* are directed laterally. This is partly due to the angled proximal articular surfaces of the unguals, where the medial edges extend further proximally than their lateral counterparts (Figs. 11–14), in addition to the beveled articulation between the unguals and adjoining proximal phalanges as is described for most sauropods (Bonnan, 2005; Hatcher, 1901). The roughened and pitted tips of the unguals (Figs. 11L, 12J–K) have been noted in other sauropods: *Camarasaurus* (Ostrom and McIntosh, 1966:241), an unnamed titanosauriform pes from Siberia (Averianov et al., 2002), *Apatosaurus louisae* (Gilmore, 1936), *Opisthocoelicaudia* (Borsuk-Bialynicka, 1977), and in general (Bonnan, 2005); nonetheless the details of this feature have rarely been illustrated for sauropod unguals (but see Canudo et al., 2008). In *Rhoetosaurus*, the ungual of the hallux is as long as Mt-I, distinguishing *Rhoetosaurus*, *Antetonitrus*, and other sauropods from basal sauropodomorph outgroups and *Vulcanodon* (Wilson and Sereno, 1998; Yates and Kitching, 2003). However, the ungual/metatarsal ratio of the first digit in *Shunosaurus*, *Cetiosauriscus*, and neosauropods is much larger than in *Rhoetosaurus*. Similarities in the phalangeal count as well as metatarsal morphology underscore the plesiomorphic similarities between *Rhoetosaurus* and the eusauropods *Shunosaurus* and *Omeisaurus*.

PHYLOGENETIC ANALYSIS

Character Matrix

To assess the phylogenetic relationships of *Rhoetosaurus* amongst sauropods, we utilized a previous character matrix (Harris, 2006; 331 characters, 30 operational taxonomic units [OTU]). Based on this study and a character survey of the remaining material of QM F1659, *Rhoetosaurus* was scored for 83 characters (70.3% missing information) following modifications to the Harris matrix (Appendix 1).

Into the matrix of Harris (2006) we incorporate *Tazoudasaurus* (Allain and Aquesbi, 2008) and *Spinophorosaurus* (Remes et al., 2009), two fairly complete Early–Middle Jurassic sauropods, both of which bear upon phylogenetic reconstruction of early sauropods. Their positions were previously analyzed using the character list of Wilson (2002; 234 characters) with scoring adjustments, so they have been re-scored here for the modified Harris matrix (Appendix 1). We significantly revamped the character scoring of *Barapasaurus* based upon new information (Upchurch et al., 2007; Bandyopadhyay et al., 2010), as well as making few scoring changes to several other taxa (listed in Appendix 1). Prosauropoda, an outgroup in the Harris matrix, was removed because it is paraphyletic and includes early sauropods (Upchurch et al., 2007). We retain Theropoda as an outgroup but acknowledge that taxa used to originally score this OTU in previous studies (*Eoraptor* and *Herrerasaurus*) may not constitute a monophyletic clade exclusive to sauropodomorphs (e.g., Upchurch et al., 2007). Given the morphological disparity and phylogenetic distance between *Eoraptor/Herrerasaurus* and our sauropod ingroup taxa, the inclusion of ‘Theropoda’, unchanged from Harris (2006), is assumed not to influence phylogenetic reconstruction of sauropods here. We have deleted four characters, but added two new characters to the Harris matrix, and emended the coding of four other characters. We list and score the deleted

characters by their original numbering order (in Harris, 2006) in our matrix (e.g., Appendix 1) but simply inactivated them prior to cladistic searching.

Analyses and Results

All 31 ingroup taxa were analyzed for 329 characters in T.N.T. 1.1 (Goloboff et al., 2003). A heuristic search (1000 replicates in ‘Traditional search’ with TBR branch swapping) revealed eight most-parsimonious trees of 841 steps, with consistency index (CI) of 0.488 and retention index (RI) of 0.626. Although we attained 1–3 fewer most-parsimonious trees performing driven searches (minimum length sought five times) under the various ‘New Technology search’ algorithms, the construction of the strict consensus from these is identical to that recovered from the ‘Traditional search’ (Fig. 18).

Within the framework of our data, *Vulcanodon* is the most basal divergence. This is followed successively by: (1) *Tazoudasaurus* + *Spinophorosaurus*; (2) *Barapasaurus*; (3) *Rhoetosaurus*; (4) *Shunosaurus*; (5) *Patagosaurus*; and (6) more-derived sauropods (Fig. 18). Thus *Rhoetosaurus* is nested outside Eusauropoda (we use a node-based definition: the *Shunosaurus lii* + *Saltasaurus loricatus* clade), but is securely within Gravisauria (Allain and Aquesbi, 2008). Previously, Harris could not reveal any resolution among most non-neosauropods in

his strict consensus tree (Harris, 2006:fig. 5A). It appears that the inclusion of new taxa (*Rhoetosaurus*, *Tazoudasaurus*, and *Spinophorosaurus*) and additional scoring for others (e.g., *Barapasaurus*) has improved branching topology along the non-neosauropod stem, even though we retain a trichotomy between *Mamenchisaurus*, *Losillasaurus*, and remaining taxa.

How well supported are these pre-Neosauropoda nodes? Bremer support here is weak, with most nodes including Neosauropoda, collapsing with one additional step (Fig. 18). In contrast, most internal nodes of Neosauropoda, especially in Diplodocoidea, are relatively better supported. Permutation of the characters (jackknifing; probability of character removal = 0.36 in 1000 resamples; Fig. 18) further shows up many clades with low resampling frequencies (e.g., *Tazoudasaurus* + *Spinophorosaurus*, *Rhoetosaurus* + Eusauropoda, or *Jobaria* placed within Macronaria are close to lacking support altogether). As to be expected, the topology of the neosauropod apex of the strict consensus is similar to the one obtained by Harris, and shows relatively strong internal support.

We measured the strengths of several alternative topologies derivable from the current data set as models of competing phylogenetic hypotheses. Based on the results of the initial analysis (Fig. 18), key areas of interest we explore cover the interrelationships of *Rhoetosaurus* among gravisaurs/basally branching eusauropods, and of the weak support for node

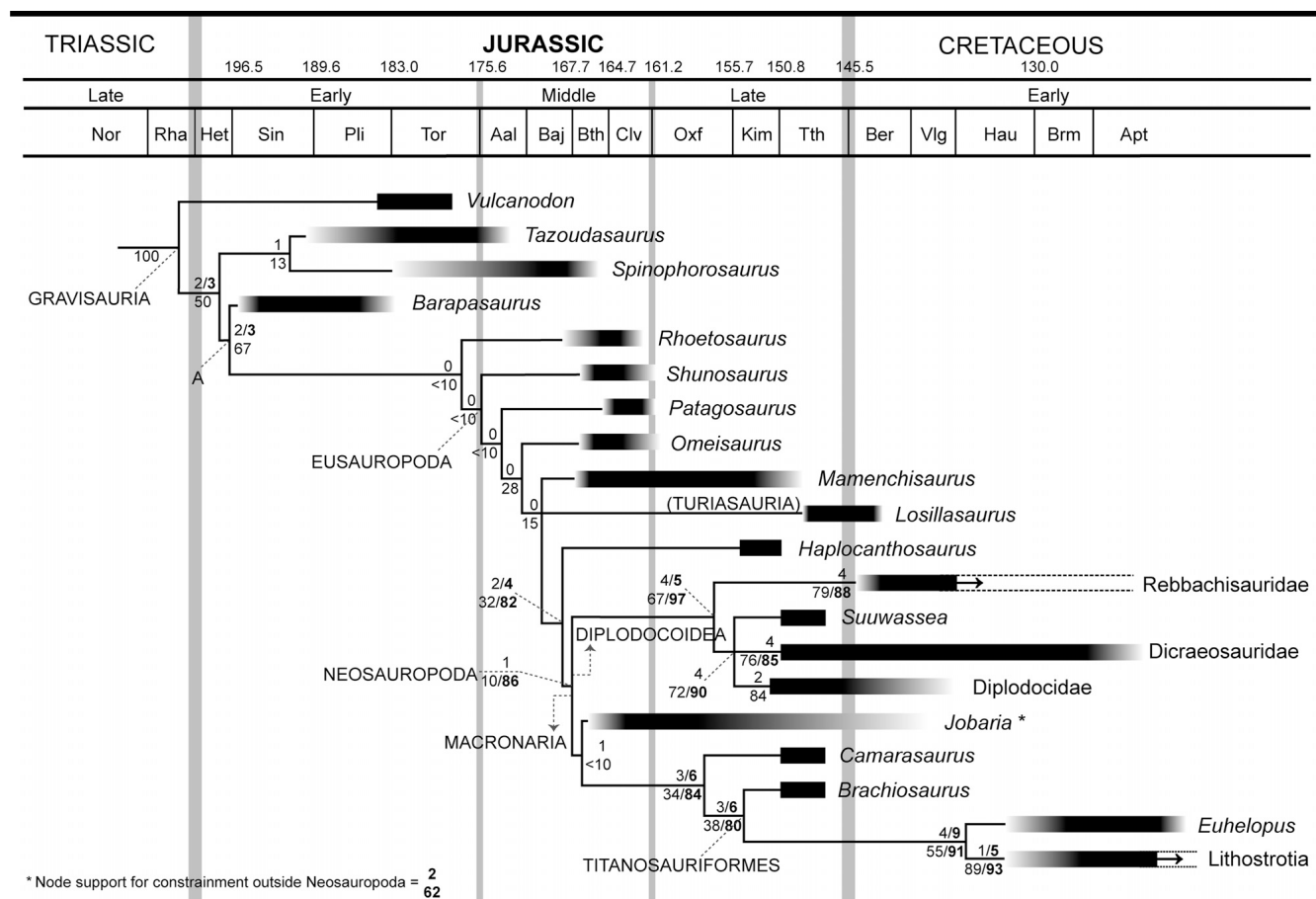


FIGURE 18. Strict consensus stratocladogram of 8 MPTs (length = 841), produced from 1000 heuristic replications of the modified data set of Harris (2006), showing phylogenetic relationships of *Rhoetosaurus*. Numbers next to nodes indicate support: top row values are Bremer decay indices; bottom row values are jackknife resampling frequencies ($p = 0.36$; 1000 replicates); values in bold font are equivalent Bremer and jackknife values under constraint of *Jobaria* outside of Neosauropoda. The OTUs comprising Lithostrotia, Diplodocidae, Dicraeosauridae, and Rebbachisauridae have been collapsed for simplicity. Time scale based on Gradstein et al. (2004). Faded portions of bars represent uncertainty in ages of strata from which the OTUs derive—see Table 2S of Supplementary Data for sources of information concerning stratigraphic age data for taxa.

TABLE 2. Alternative hypotheses (topological constraints) and Templeton test results.

Constraint	No. MPTs	TL MPTs	+ steps	TL con	C _{alt} /C	T _s /T _{H0}	P	Comment
Unconstrained tree	8	841	0	857	—	—	—	—
1. <i>Shunosaurus</i> , (<i>Barapasaurus</i> , Rh, Pa + others)	16	842	1	861	5/14	37.5/52.5	0.301	Cannot reject
2. <i>Jobaria</i> outside of Neosauropoda	8	842	1	858	3/7	12/14	0.777	Cannot reject
3. <i>Vulcanodon-Tazoudasaurus-Spinophorosaurus</i> paraphyletic (removal of Ta-Sp monophly)	32	842	1	865	2/12	13/39	0.024	Significant
4. <i>Shunosaurinae</i> , sensu McIntosh (1990) (Sh + Rh + Om)	16	858	17	889	2/35	35/315	<0.0001	Significant
5. <i>Rhoetosaurus</i> + <i>Shunosaurus</i> clade	18	842	1	866	5/21	66/115.5	0.052	Cannot reject; close to significance
6. <i>Rhoetosaurus</i> in Neosauropoda	36	846	5	872	6/27	84/189	0.004	Significant
7. <i>Rhoetosaurus</i> closer to Neosauropoda than any of <i>Shunosaurus</i> , <i>Barapasaurus</i> , or <i>Patagosaurus</i>	36	844	3	871	6/26	81/175.5	0.006	Significant
8. Clade of Gondwanan Middle Jurassic sauropods (Sp + Rh + Pa)	8	847	6	863	6/18	57/85.5	0.165	Cannot reject

Abbreviations: TL MPTs, tree length of each MPT; + steps, number of extra steps between MPTs of constrained trees and MPTs of unconstrained trees; TL con, tree length of strict consensus of MPTs (TL increases because of polytomies, and by default TNT obtains TL on the ‘hard’ polytomy assumption); C_{alt}, number of character changes that support the alternative topology; C, number of characters that change between constrained and unconstrained searches (hence, number of character changes supporting original topology = C – C_{alt}); T_s, the test statistic, is the Wilcoxon summed rank of n-values that favor the alternative topology; T_{H0}, the expected test statistic, describing different topologies being perfectly accommodated by the same data (= null hypothesis); P, P-value, two tailed probability (significance ≤ 0.005) of rejecting H₀; Om, *Omeisaurus*; Pa, *Patagosaurus*; Rh, *Rhoetosaurus*; Sh, *Shunosaurus*; Sp, *Spinophorosaurus*; Ta, *Tazoudasaurus*.

Neosauropoda. Each competing hypothesis was simulated by enforcing topological constraints (Table 2) prior to searching, from which a consensus was derived. Changes in character steps between the constrained and original consensus were compared using a Templeton test (described in Larson, 1994; Wilson, 2002:234) to evaluate if the data set could support the alternative topologies. Character step scores for the consensus trees were exported from T.N.T. into Excel, where we executed the Wilcoxon signed-ranked test (with XLSTAT 2010.5.08; Addinsoft) to yield a two-tailed probability statistic used to retain or reject alternative topologies (Table 2). We discuss the implications of these competing hypotheses below.

DISCUSSION

Evolutionary Trends in Phalangeal Counts

The pattern of reduction in phalanges and expression of ununiform terminal phalanges is strongly correlated with sauropod phylogeny (Table 1), accounting for anomalous observations (e.g., CM 89, *Dyslocosaurus*, FMNH 241–50; comments in Table 1). Early non-gravisaurian sauropods (e.g., *Blikanasaurus*, *Gongxianosaurus*) had four and five phalanges on digits III and IV, respectively, and at least four unguals across the pes. Basally branching eusauropods had a reduced phalangeal count in digit IV to three units, but retained four pedal unguals, which was only reduced to three unguals among more nested non-neosauropods. Reduction in digit III to three or fewer phalanges occurred several times among nested non-neosauropods and diplodocoids, but appears to have been definitely reduced to two units among nested titanosaurs (González Riga et al., 2008). Phalangeal formulas can thus be considered an indicator of phylogenetic trends within sauropods, and a practical tool for gauging phylogeny of incomplete specimens.

Atrophied phalanges of *Rhoetosaurus*, when compared to those of other sauropods, shed light on the pattern by which phalanges are lost. The penultimate phalanges of digits II–IV in *Rhoetosaurus* are compressed nubbins, whereas in basal sauropods such as *Blikanasaurus*, *Gongxianosaurus*, and *Vulcanodon*, these phalanges are unreduced, being comparatively proximodistally longer (Raath, 1972; Galton and Van Heerden, 1998; He et al., 1998). In *Rhoetosaurus*, phalanx III-2 is an in situ pre-

served element that is pinched laterally, and is for that reason constrained only medially between III-1 and III-3 (Fig. 13). The only comparable example to this in the literature is phalanx III-2 of *Janenschia* (Bonaparte et al., 2000:fig. 8A), but here it is restricted laterally, opposite to the condition in *Rhoetosaurus*. The positioning of this bone, however, is probably assumed in the reconstruction of *Janenschia*. Phalanx II-2 in *Rhoetosaurus* is also wedge-shaped, narrowing laterally (Fig. 12), whereas I-1 and IV-2, although not pinched, are asymmetrical (Figs. 11, 14). Hatcher proposed that sauropod phalanges become atrophied through functional disuse (1901:51). Evolutionary reduction in phalangeal numbers in sauropods seems to be a stepwise process, where individual units are: first, shortened; second, become asymmetrical and wedge-shaped; third, shift medially; before fourth, finally being lost.

Phylogenetic Relationships of *Rhoetosaurus*

Eusauropod Interrelationships—*Rhoetosaurus* was recovered as a non-eusauropod in the heuristic search consensus but its positioning relative to *Shunosaurus* and neighboring branches appears equivocal given the weak resampling support at these nodes (Fig. 18). Constraining *Rhoetosaurus* within Eusauropoda by way of forcing *Shunosaurus* outside the *Barapasaurus* + neosauropod group produces most-parsimonious trees (MPTs) only one step longer than the original analysis (Table 2, constraint 1). The Templeton test result indicates that constrained topology number 1 does not represent a statistically worse explanation, and cannot be rejected with the current data set. Interestingly, *Rhoetosaurus* and *Barapasaurus* form a consensus clade within Eusauropoda under constraint 1, united by a transversely elongate astragalus (character 306).

Most previous analyses have recovered *Shunosaurus* basal to *Barapasaurus* (Wilson and Sereno, 1998; Allain and Aquesbi, 2008; Remes et al., 2009), hence pushing the latter taxon into Eusauropoda. However, our result supports the inverted positions of these two sauropods (corroborating Upchurch et al., 2007; Bandyopadhyay et al., 2010), and this also appears stratigraphically more likely (Fig. 18; see 2S in Supplementary Data). Consequently, eusauropods may be inferred to have arisen as recently as the early Middle Jurassic.

A more-inclusive clade of gravisauroian sauropods that excludes *Spinophorosaurus*, *Vulcanodon*, and *Tazoudasaurus* is relatively better supported by the data, and regardless of the true topology between *Barapasaurus*, *Rhoetosaurus*, and *Shunosaurus*, it is apparent that *Rhoetosaurus* belongs within this unnamed clade (Fig. 18, ‘node A’).

Influences of ‘Wildcard Taxa’—Some OTUs strongly influence the overall phylogenetic reconstruction presented here, often due to the distribution of scored characters for them (incompleteness or concerted scoring). *A priori* removal of *Rhoetosaurus*, which has approximately 70% missing information in the modified matrix, inflicts a reversed paraphyletic positioning between *Barapasaurus* and *Shunosaurus* (and improved support; recalculated jackknife resampling frequencies are approximately 1.5–2.5 times better for all pre-neosauropod nodes). Because *Shunosaurus* is near-completely known, this result is best explained by the comparative distribution of some scores between *Barapasaurus* and *Rhoetosaurus*. Presently scored characters in *Rhoetosaurus* are concerted in the caudal vertebrae and hind limb. However in *Barapasaurus*, the pes is less completely known, whereas several hind limb characters are unscored because they are disarticulated from multiple individuals (Bandyopadhyay et al., 2010). Additional information on either or both taxa would likely stabilize this area of the tree.

Another influential taxon is *Haplocanthosaurus* (Wilson and Sereno, 1998:54), which appears to specifically control flagellicaudata topology in this work. Whitlock and Harris (2010) recently augmented known information for the probable dicraeosaurid *Suuwassea* (Appendix 1), but noted its topological position in Flagellicaudata remained unchanged from Harris (2006) unless three novel characters were introduced (two of them are dicraeosaurid synapomorphies). *A priori* removal of *Haplocanthosaurus* in our data set resolves a diphylectic Flagellicaudata by migrating *Suuwassea* into Dicraeosauridae.

We achieved poor Bremer and resampling support for node Neosauropoda, and we identify *Jobaria* as a wildcard taxon causing this. Our consensus resolves *Jobaria* as the basal-most macronarian, but the nodes Camarasauromorpha and Titanosauriformes lack resampling support in this arrangement, and Somphospondyli (here represented by *Euhelopus* + *Lithostrotia*) is recovered in only a bare majority of iterations (55%). The Templeton test cannot reject the alternative placement of *Jobaria* outside Neosauropoda (Table 2, constraint 2), which is only one step longer and supported by nearly half the character step changes between the original and alternative topologies. Despite the suboptimal length, this alternative not only leads to improved node support, but also shortens ghost lineages at the base of Diplodocoidea and Macronaria originally resulting from the older stratigraphic age of *Jobaria*. The alternative arrangement produces substantially increased jackknife support for the *Haplocanthosaurus*-*Jobaria*-Neosauropoda clade and all its internal nodes, whereas Bremer support for each macronarian clade is doubled (or greater) (Fig. 18; support values in bold). Clearly *Jobaria* is a crucial taxon for understanding neosauropod evolution, but requires renewed consideration of its character data in light of its emplacement into newer phylogenetic matrices.

Finally, confounding phylogenies may arise from causes other than incompletely known taxa. Our consensus below ‘node A’ (Fig. 18) yielded a *Spinophorosaurus*-*Tazoudasaurus* monophly, contrasting with Allain and Aquesbi (2008) who found a *Tazoudasaurus*-*Vulcanodon* clade, and Remes et al. (2009), who found the three taxa in serial paraphly. Our Templeton test result rejects the latter arrangement (Table 2, constraint 3), whereas Remes et al. could not reject the *Spinophorosaurus*-*Tazoudasaurus* clade in their analysis (Remes et al., 2009:table 3). We attribute these contradictory results to differences in the size of the data sets (the Harris matrix includes about 100 more

characters absent in the other two data sets), and coding assumptions (ordered change was imposed on many characters in Remes et al. [2009] that were previously unorderd in Wilson [2002]).

Alternative Arrangements and Paleobiogeography—Some early studies offered comments on the affinities of *Rhoetosaurus*, mainly based on comparisons of vertebral anatomy. Longman (1927a, 1927b) remarked that the tail of *Rhoetosaurus* resembled that of another Middle Jurassic sauropod, *Cetiosaurus oxoniensis*, lacked affinities to diplodocids, and eventually classified *Rhoetosaurus* in Camarasauridae (sensu ‘Cetiosauridae,’ Longman, 1926). Cabrera (1947) suggested *Rhoetosaurus* might have affinities with *Amygdalodon* (recognised as a ‘cetiosaurid’ at the time) because of their common Gondwanan range, but also pointed out several differences between the two genera. These early papers forwarded very general statements of phylogeny, to which we do not offer any further comment.

McIntosh (1990) grouped *Rhoetosaurus* with *Shunosaurus* and *Omeisaurus* in a new subfamily, Shunosaurinae, within Cetiosauridae, remarking that *Rhoetosaurus* possessed derived features separating it from *Vulcanodon*. Molnar and Thulborn (in Grant-Mackie et al., 2000) considered *Rhoetosaurus* similar to *Shunosaurus*. A sister-group relationship between *Rhoetosaurus* and *Shunosaurus* was not supported by the results of our analysis. However, in order to investigate this idea further, an analysis was run in which ‘Shunosaurinae’ sensu McIntosh (1990) was enforced (Table 2, constraint 4). In the context of our data set, this arrangement can be rejected with confidence ($P < 0.0001$). Alternatively, a restricted *Rhoetosaurus*-*Shunosaurus* clade (constraint 5) results in MPTs only one step longer than the unconstrained MPTs. Although this topology cannot be statistically rejected, the P -value (0.052) straddles the cut off for significance, and indicates the data set can almost reject this arrangement. Upchurch (1995:374) hinted that the basis of McIntosh’s grouping of *Rhoetosaurus* within Shunosaurinae, with forms such as *Omeisaurus* and *Shunosaurus*, rested upon a supposedly similar forked morphology of the non-proximal hemal arches. Close scrutiny of the non-proximal hemal arch morphology of QM F1659 indicates they are not particularly close in form to those of the Asian sauropods, and do not form a forked morphology. Upchurch (1995) also queried if *Rhoetosaurus* actually possessed the forked condition of *Shunosaurus* and diplodocids, and since then, the feature has been identified in a broad array of sauropods, including *Barapasaurus* and *Tazoudasaurus* (Bandyopadhyay et al., 2010).

Upchurch (1995:374) identified *Rhoetosaurus* as ‘Neosauropoda incertae sedis.’ A more recent study could not assign *Rhoetosaurus* more specifically than to Sauropoda incertae sedis, but this same work indicated a closer relationship with neosauropods than to basally divergent eusauropods (Upchurch et al., 2004a:261, 299). The Templeton test rejects an alternative *Rhoetosaurus*-Neosauropoda grouping as well as *Rhoetosaurus* placed topologically nearer to neosauropods than *Barapasaurus*, *Shunosaurus*, and *Patagosaurus* (Table 2, constraints 6–7).

Prior assessments of affinity between *Rhoetosaurus* with *Shunosaurus* or with multiple East Asian eusauropods were based on few morphological similarities, some of which are now known widely among pre-Late Jurassic sauropods. It is unsurprising that the Templeton test rejected the monophly of Shunosaurinae, given that all analyses since Upchurch (1998) found *Shunosaurus* and *Omeisaurus* were sequentially paraphyletic towards neosauropods. The disparate paleogeographic locations between the east Asian sauropod fauna and the Injune Creek Group, coupled with widespread climatic barriers between southern Gondwana and Laurasia during much of the Jurassic (Sellwood and Valdes, 2008), are added grounds for doubting the *Rhoetosaurus*-‘Shunosaurinae’ link.

Although far less parsimonious (six extra steps), a clade of exclusively post-Toarcian Gondwanan sauropods (*Rhoetosaurus*,

Spinophorosaurus, and *Patagosaurus*) cannot be statistically rejected by the data set (Table 2, constraint 8). Inclusion of *Spinophorosaurus* from northern Gondwana within a nexus of otherwise southern Gondwanan taxa depends on its age (presently imprecise) relative to the timing of the recession of the Central Gondwanan Desert (Remes et al., 2009). Further work and additional discoveries are required to examine potential monophyly among southern Gondwanan sauropods.

A high proportion of missing data in *Rhoetosaurus* and low node support among early eusauropods emphasizes the need to be cautious regarding the current position of *Rhoetosaurus*. Upchurch noted that the anatomy of thoracic vertebrae in *Rhoetosaurus* is characteristic of nested eusauropods/neosauropods (Upchurch, 1995), implying that at least this alternative hypothesis (constraint 7), although rejected for the present, deserves closer scrutiny if and when more information on *Rhoetosaurus* becomes available. Pending such reappraisal, the current monophyly of *Rhoetosaurus* + Eusauropoda, with *Barapasaurus* basal to this clade, is supported by three synapomorphies: fourth trochanter situated on the caudomedial margin of the femoral body (character 280, also in *Spinophorosaurus*); tibial cnemial crest reduced to a low ridge (character 292, also in *Vulcanodon*); metatarsal I with ventromedially angled proximal articular surface, relative to metatarsal body in cranial view (character 311, reversed in *Patagosaurus*).

Morphofunctional Considerations

Bonnan (2005) noted that beveled metatarsophalangeal ginglymi contribute slightly toward directing pedal digits laterally in neosauropods. However, the chief reason for the lateral orientation is caused by articular ginglymi among the terminal-most phalanges being beveled and oriented craniolaterally. The ginglymi in digits of *Rhoetosaurus* are beveled only terminally within the pes, not at the metatarsophalangeal transition, which may support the staggered accumulation of pedal traits among gravisaurians preceding Neosauropoda. Some stages in the process of phalangeal reduction (see foregoing discussion on evolution of phalangeal loss) also contribute toward laterally directing unguis, i.e., the medial, rather than lateral, shifting of already reduced non-terminal phalanges imposes additional sloping in the ginglymi.

Pedal unguals are understood to be capable of considerable extension/flexion motion (Bonnan, 2005), and perhaps even adhesion/abduction (although no quantitative data for the latter exists; Gallup, 1989). Ungual movements, coupled with the re-orientation of claws laterally, are used to support ideas of nest excavation via hind-feet-first digging (Hildebrand, 1985; Gallup, 1989) or substrate gripping as a means of improving traction during locomotion (Gallup, 1989; Bonnan, 2005). Even though assessment of these hypotheses is outside the scope of this work, we suggest that reduction in ungual number and phalanges in derived titanosauriforms (Table 1; González Riga et al., 2008) relate to earlier acquired morphological innovations among macronarians, or even neosauropods.

The broadened pelvic region and modified femoral anatomy of titanosauriforms have been linked to wide-gauge trackway production (Wilson and Carrano, 1999). Alternatively, wide-gauge trackways may simply correlate to larger neosauropod trackmakers that have a wider locomotor gauge catering for their relatively anterior center of body mass (Henderson, 2006). If pedal claws functioned in providing traction control, as preferred by Bonnan (2005), then their retention with high biomechanical capability would have been crucial in providing stability control for early graviportal sauropodomorphs. The later transformation to a wide-gauge potentially de-emphasized the functional role of pedal claws, reducing their need to provide stability control among neosauropods. Conceivably, the evolution of a less ‘tipsy’ gait through additional anatomical transformations in the pelvis

among early titanosauriforms preceded the further reduction of pedal phalanges.

CONCLUSION

Based solely on the hind limb, *Rhoetosaurus* can be distinguished from contemporary sauropods by a multitude of osteological differences (Figs. 15–16), reaffirming how incomplete specimens can yield a wealth of data. Despite this, we recover *Rhoetosaurus* in an intermediate but weakly supported position within Gravisauria, which is probably due to the underscored mix of derived and plesiomorphic traits. Some pedal traits considered characteristic of diplodocids (Fig. 17) are realized to have wider distribution among sauropods (Canudo et al., 2008). Additional to the materials described herein, much information exists in the remaining hypodigm, which in future studies would serve to refine phylogenetic hypotheses concerning *Rhoetosaurus*.

ACKNOWLEDGMENTS

This research was not possible without the efforts of local paleontologists who contributed to recovery of *Rhoetosaurus* specimens in the 1970s–1990s. Amongst these we thank Drs. A. Bartholomai, R. Molnar, T. Rich, A. Rozefelds, T. Thulborn, A. Warren, and X. Zhao. In particular, the late Dr. Mary Wade was instrumental for her role in the recovery of the pes. For access to specimens in their care at Queensland Museum, we thank K. Spring and S. Hocknull. D. Lewis produced moulds of the *Rhoetosaurus* pes, which we cast with the assistance of M. Herne and R. Berrell. T. Rich provided unpublished diary notes pertaining to the type locality. For use of photographs or other data, or for relevant discussions, we thank A. Bartholomai, L. Beirne, M. Herne, T. Ikejiri, J. McKellar, R. Molnar, P. Rose, and the late Norman Timms (who provided a recollection of the original discovery). We appreciate the feedback given by the anonymous reviewers, M. D’Emic, and co-senior editor P.M. Barrett. This research was funded in part by the Australian Research Council (LP0347332 and LP0776851) and The University of Queensland (to S.W.S.), in association with Longreach Regional Council, Winton Shire Council, Land Rover Australia, the Queensland Museum, and a Rea Postdoctoral Fellowship (to S.W.S.) at Carnegie Museum of Natural History.

LITERATURE CITED

- Alifanov, V. R., and A. O. Averianov. 2003. *Ferganasaurus verzilini*, gen. et sp. nov., a new neosauropod (Dinosauria, Saurischia, Sauropoda) from the Middle Jurassic of Fergana Valley, Kirghizia. Journal of Vertebrate Paleontology 23:358–372.
- Allain, R., and N. Aquesbi. 2008. Anatomy and phylogenetic relationships of *Tazoudasaurus naimi* (Dinosauria, Sauropoda) from the late Early Jurassic of Morocco. Geodiversitas 30:345–424.
- Allain, R., P. Taquet, B. Battail, J. Dejax, P. Richir, M. Veran, F. Limon-Duparcmeur, R. Vacant, O. Mateus, P. Sayarath, B. Khenthavong, and S. Phouyavong. 1999. Un nouveau genre de dinosaure sauroptéde de la formation des Gres supérieurs (Aptien-Albien) du Laos. Comptes Rendus de l’Academie des Sciences, (Serie II). Sciences de la Terre et des Planètes 329:609–616.
- Averianov, A. O., A. V. Voronkevich, E. N. Maschenko, S. V. Leshchinskii, and A. V. Fayngertz. 2002. A sauropod foot from the Early Cretaceous of western Siberia, Russia. Acta Palaeontologica Polonica 47:117–124.
- Bandyopadhyay, S., D. D. Gillette, S. Ray, and D. P. Sengupta. 2010. Osteology of *Barapasaurus tagorei* (Dinosauria: Sauropoda) from the Early Jurassic of India. Palaeontology 53:533–569.
- Bartholomai, A. 1966. Fossil footprints in Queensland. Australian Natural History 15:147–150.
- Bedell, M. W., Jr., and D. L. Trexler. 2005. First articulated manus of *Diplodocus carnegii*; pp. 302–320 in V. Tidwell and K. Carpenter (eds.), Thunder-Lizards: The Sauropodomorph Dinosaurs. Indiana University Press, Bloomington and Indianapolis, Indiana.
- Bonaparte, J. F. 1986. Les dinosaures (carnosaures, allosauridés, sauroptédes, cétiosauridés) du Jurassique moyen de Cerro Cónedor

- (Chubut, Argentine). *Annales de Paleontologie* 72:247–289, 326–386.
- Bonaparte, J. F., W.-D. Heinrich, and R. Wild. 2000. Review of *Janenschia* Wild, with the description of a new sauropod from the Tendaguru beds of Tanzania and a discussion on the systematic value of procoelous caudal vertebrae in the Sauropoda. *Palaeontographica Abteilungen A* 256:25–76.
- Bonnan, M. F. 2000. The presence of a calcaneum in a diplodocid sauropod. *Journal of Vertebrate Paleontology* 20:317–323.
- Bonnan, M. F. 2005. Pes anatomy in sauropod dinosaurs: implications for functional morphology, evolution, and phylogeny; pp. 346–380 in V. Tidwell and K. Carpenter (eds.), *Thunder-Lizards: The Sauropodomorph Dinosaurs*. Indiana University Press, Bloomington and Indianapolis, Indiana.
- Borsuk-Bialynicka, M. 1977. A new camarasaurid sauropod *Opisthocoelicaudia skarzynskii* gen. n., sp. n. from the Upper Cretaceous of Mongolia. *Palaeontologia Polonica* 37:5–64.
- Cabrera, A. 1947. Un saurópodo nuevo del Jurásico de Patagonia. Notas del Museo de la Plata 12:1–17.
- Calvo, J. O., and L. Salgado. 1995. *Rebbachisaurus tessonei* sp. nov. a new Sauropoda from the Albian-Cenomanian of Argentina; new evidence on the origin of the Diplodocidae. *Gaia* 11:13–33.
- Canudo, J. I., R. Royo-Torres, and G. Cuenca-Bescos. 2008. A new sauropod: *Tastavinsaurus sanzi* gen. et sp. nov. from the Early Cretaceous (Aptian) of Spain. *Journal of Vertebrate Paleontology* 28:712–731.
- Coombs, W. P., Jr., and R. E. Molnar. 1981. Sauropoda (Reptilia, Saurischia) from the Cretaceous of Queensland. *Memoirs of the Queensland Museum* 20:351–373.
- Cooper, M. R. 1984. A reassessment of *Vulcanodon karibaensis* Raath (Dinosauria: Saurischia) and the origin of the Sauropoda. *Palaeontologia Africana* 25:203–231.
- Fraas, E. 1908. Ostafrikanische Dinosaurier. *Palaeontographica* 55:105–144.
- Gallup, M. R. 1989. Functional morphology of the hindfoot of the Texas sauropod *Pleurocoelus* sp. indet. *Geological Society of America, Special Paper* 238:71–74.
- Galton, P. M., and P. Upchurch. 2004. Prosauropoda; pp. 232–258 in D. B. Weishampel, P. Dodson, and H. Osmólska (eds.), *The Dinosauria*, 2nd edition. University of California Press, Berkeley, California.
- Galton, P. M., and J. Van Heerden. 1998. Anatomy of the prosauropod dinosaur *Blikanasaurus cromptoni* (Upper Triassic, South Africa), with notes on the other tetrapods from the lower Elliot Formation. *Paläontologische Zeitschrift* 72:163–177.
- Galton, P. M., J. Van Heerden, and A. M. Yates. 2005. Postcranial anatomy of referred specimens of the sauropodomorph dinosaur *Melanorosaurus* from the Upper Triassic of South Africa; pp. 1–37 in V. Tidwell and K. Carpenter (eds.), *Thunder-Lizards: The Sauropodomorph Dinosaurs*. Indiana University Press, Bloomington and Indianapolis, Indiana.
- Gilmore, C. W. 1932. On a newly mounted skeleton of *Diplodocus* in the United States National Museum. *Proceedings of the United States National Museum* 81:1–21.
- Gilmore, C. W. 1936. Osteology of *Apatosaurus*, with special reference to specimens in the Carnegie Museum. *Memoirs of the Carnegie Museum* 11:175–300.
- Goloboff, P. A., J. S. Farris, and K. C. Nixon. 2003. T.N.T.: Tree Analysis Using New Technology. Willi Hennig Society Edition 1.1. Willi Hennig Society. <http://www.zmuc.dk/public/phylogeny/TNT/>. Accessed October 30, 2010.
- González Riga, B. J., J. O. Calvo, and J. D. Porfiri. 2008. An articulated titanosaur from Patagonia (Argentina): new evidence of neosauropod pedal evolution. *Palaeoworld* 17:33–40.
- Gradstein, F. M., J. G. Ogg, and A. G. Smith (eds.). 2004. *A Geologic Time Scale 2004*. Cambridge University Press, Cambridge, U.K., 589 pp.
- Grant-Mackie, J. A., Y. Aita, B. E. Balme, H. J. Campbell, A. B. Challinor, D. A. B. MacFarlan, R. E. Molnar, G. R. Stevens, and R. A. Thulborn. 2000. Jurassic palaeobiogeography of Australasia; pp. 311–354 in A. J. Wright and G. C. Young (eds.), *Palaeobiogeography of Australian Faunas and Floras*. Association of Australasian Palaeontologists, Canberra.
- Green, P. M., D. C. Carmichael, T. J. Brain, C. G. Murray, J. L. McKellar, J. W. Beeston, and A. R. G. Gray. 1997. Lithostratigraphic units in the Bowen and Surat basins, Queensland; pp. 41–108 in P. M. Green (ed.), *The Surat and Bowen Basins South-East Queensland*. Queensland Department of Mines and Energy, Brisbane.
- Harris, J. D. 2006. The significance of *Suuwassea emilieae* (Dinosauria: Sauropoda) for flagellicaudatan intrarelationships and evolution. *Journal of Systematic Paleontology* 4:185–198.
- Harris, J. D. 2007. The appendicular skeleton of *Suuwassea emilieae* (Sauropoda: Flagellicaudata) from the Upper Jurassic Morrison Formation of Montana (USA). *Geobios* 40:501–522.
- Hatcher, J. B. 1901. *Diplodocus* (Marsh): its osteology, taxonomy, and probable habits, with a restoration of the skeleton. *Memoirs of the Carnegie Museum* 1:1–63.
- He, X., K. Li, and K. Cai. 1988. [The Middle Jurassic Dinosaurian Fauna from Dashanpu, Zigong, Sichuan. IV. The Sauropod Dinosaurs 2. *Omeisaurus tianfuensis*.] Sichuan Scientific and Technological Publishing House, Chengdu, Sichuan, 143 pp. [Chinese with English summary]
- He, X., C. Wang, S. Liu, F. Zhou, T. Liu, K. Cai, and B. Dai. 1998. [A new species of sauropod from the Early Jurassic of Gongxian Co., Sichuan]. *Acta Geologica Sichuan* 18:1–7. [Chinese with English summary]
- Heathcote, J. 2002. The anatomy and phylogeny of *Cetiosauriscus stewarti*: a Middle Jurassic sauropod from Peterborough, England. M.Sc. thesis, University of Cambridge, Cambridge, U.K., 65 pp.
- Helby, R., R. Morgan, and A. D. Partridge. 1987. A palynological zonation of the Australian Mesozoic; pp. 1–94 in P. A. Jell (ed.), *Studies in Australian Mesozoic Palynology*. Association of Australasian Palaeontologists, Sydney.
- Henderson, D. M. 2006. Burly gaits: centers of mass, stability, and the trackways of sauropod dinosaurs. *Journal of Vertebrate Paleontology* 26:907–921.
- Hildebrand, M. 1985. Digging of quadrupeds; pp. 89–109 in M. Hildebrand, D. M. Bramble, K. F. Liem, and D. B. Wake (eds.), *Functional Vertebrate Morphology*. The Belknap Press of Harvard University Press, Cambridge, Massachusetts, and London.
- Hocknull, S. A., M. A. White, T. R. Tischler, A. G. Cook, N. D. Calleja, T. Sloan, and D. A. Elliott. 2009. New mid-Cretaceous (latest Albian) dinosaurs from Winton, Queensland, Australia. *PLoS ONE* 4:e6190.
- Huene, F. von. 1932. Die fossile reptil-ordnung Saurischia, ihre Entwicklung und geschichte. Monographien zur Geologie und Palaeontologie (Serie I) 4:1–361.
- International Commission on Zoological Nomenclature. 1999. International Code of Zoological Nomenclature. 4th Edition. International Trust for Zoological Nomenclature, London, 336 pp.
- Janensch, W. 1961. Die gliedmaszen und gliedmaszengurtel der sauropoden der Tendaguru-Schichten. *Palaeontographica* (Supplement 7) 3:177–235.
- Langer, M. C. 2003. The pelvic and hind limb anatomy of the stem-sauropodomorph *Saturnalia tupiniquim* (Late Triassic, Brazil). *PaleoBios* 23:1–40.
- Larson, A. 1994. The comparison of morphological and molecular data in phylogenetic systematics; pp. 371–390 in B. Schierwater, B. Streit, G. P. Wagner, and R. DeSalle (eds.), *Molecular Ecology and Evolution: Approaches and Applications*. Birkhauser Verlag, Basel.
- Long, J. A. 1992. First dinosaur bones from Western Australia. *The Beagle, Records of the Northern Territory Museum of Arts and Sciences* 9:21–28.
- Long, J. A., and R. E. Molnar. 1998. A new Jurassic theropod dinosaur from Western Australia. *Records of the Western Australian Museum* 19:121–129.
- Longman, H. A. 1926. A giant dinosaur from Durham Downs, Queensland. *Memoirs of the Queensland Museum* 8:183–194.
- Longman, H. A. 1927a. The giant dinosaur: *Rhoetosaurus brownei*. *Memoirs of the Queensland Museum* 9:1–18.
- Longman, H. A. 1927b. Australia's largest fossil. *Australian Museum Magazine* 3:97–102.
- Longman, H. A. 1929. Palaeontological notes. *Memoirs of the Queensland Museum* 9:247–251.
- Marsh, O. C. 1878. Principal characters of American Jurassic dinosaurs. Part I. *American Journal of Science (Series 3)* 16:411–416.
- Martínez, R. D., O. Giménez, J. Rodríguez, M. Luna, and M. C. Lamanna. 2004. An articulated specimen of the basal titanosaurian (Dinosauria: Sauropoda) *Epochthosaurus sciuttoi* from the early Late Cretaceous Bajo Barreal Formation of Chubut Province, Argentina. *Journal of Vertebrate Paleontology* 24:107–120.
- McIntosh, J. S. 1990. Sauropoda; pp. 345–401 in D. B. Weishampel, P. Dodson, and H. Osmólska (eds.), *The Dinosauria*. University of California Press, Berkeley, California.

- McIntosh, J. S. 2005. The genus *Barosaurus* Marsh (Sauropoda, Diplodocidae); pp. 38–77 in V. Tidwell and K. Carpenter (eds.), Thunder-Lizards: The Sauropodomorph Dinosaurs. Indiana University Press, Bloomington and Indianapolis, Indiana.
- McIntosh, J. S., W. P. Coombs Jr., and D. A. Russell. 1992. A new diplodocid sauropod (Dinosauria) from Wyoming, U.S.A. *Journal of Vertebrate Paleontology* 12:158–167.
- McIntosh, J. S., C. A. Miles, K. C. Cloward, and J. R. Parker. 1996. A new nearly complete skeleton of *Camarasaurus*. *Bulletin of Gunma Museum of Natural History* 1:1–87.
- McKellar, J. L. 1998. Late Early to Late Jurassic palynology, biostratigraphy and palaeogeography of the Roma Shelf area, northwestern Surat Basin, Queensland, Australia. Ph.D. dissertation, The University of Queensland, Brisbane, Queensland, Australia, 515 pp.
- Molnar, R. E. 1991. Fossil reptiles in Australia; pp. 605–702 in P. Vickers-Rich, J. M. Monaghan, R. F. Baird, T. H. Rich, E. M. Thompson, and C. Williams (eds.), Vertebrate Palaeontology of Australasia. Pioneer Design Studio, and Monash University Publications Committee, Melbourne.
- Molnar, R. E., and S. W. Salisbury. 2005. Observations on Cretaceous sauropods from Australia; pp. 454–465 in V. Tidwell and K. Carpenter (eds.), Thunder-Lizards: The Sauropodomorph Dinosaurs. Indiana University Press, Bloomington and Indianapolis, Indiana.
- Ostrom, J. H., and J. S. McIntosh. 1966. Marsh's Dinosaurs—The Collections from Como Bluff. Yale University Press, New Haven, 388 pp.
- Ouyang, H., and Y. Ye. 2002. [The First Mamenchisaurian Skeleton with Complete Skull—*Mamenchisaurus youngi*]. Sichuan Scientific and Technological Publishing House, Chengdu, Sichuan, 110 pp. [Chinese with English summary]
- Padian, K. 1992. A proposal to standardize tetrapod phalangeal formula designations. *Journal of Vertebrate Paleontology* 12:260–262.
- Pol, D., and J. E. Powell. 2007. New information on *Lessemsaurus sauropoides* (Dinosauria: Sauropodomorpha) from the Upper Triassic of Argentina. *Special Papers in Palaeontology* 77:223–243.
- Raath, M. A. 1972. Fossil vertebrate studies in Rhodesia: a new dinosaur (Reptilia: Saurischia) from near the Trias-Jurassic boundary. *Arnoldia* 5(30):1–37.
- Remes, K. 2006. Revision of the Tendaguru sauropod dinosaur *Tornieria africana* (Fraas) and its relevance for sauropod paleobiogeography. *Journal of Vertebrate Paleontology* 26:651–669.
- Remes, K., F. Ortega, I. Fierro, U. Joger, R. Kosma, J. M. Marín Ferrer, Project PALDES, Niger Project SNHM, O. A. Ide, and A. Maga. 2009. A new basal sauropod dinosaur from the Middle Jurassic of Niger and the early evolution of Sauropoda. *PLoS ONE* 4:e6924.
- Rich, T. H. 1996. Significance of polar dinosaurs in Gondwana. *Memoirs of the Queensland Museum* 39:711–717.
- Rich, T. H., and P. Vickers-Rich. 2003. A Century of Australian Dinosaurs. Queen Victoria Museum and Art Gallery, Launceston, and Monash Science Centre, Monash University, Melbourne, 125 pp.
- Rich, T. H., P. Vickers-Rich, and R. A. Gangloff. 2002. Polar dinosaurs. *Science* 295:979–980.
- Rothschild, B. M., and R. E. Molnar. 2005. Sauropod stress fractures as clues to activity; pp. 381–392 in V. Tidwell and K. Carpenter (eds.), Thunder-Lizards: The Sauropodomorph Dinosaurs. Indiana University Press, Bloomington and Indianapolis, Indiana.
- Salisbury, S. W., M. C. Lamanna, and R. E. Molnar. 2006. A new titanosauriform sauropod from the mid-Cretaceous (Albian-Cenomanian) Winton Formation of central-western Queensland, Australia. *Journal of Vertebrate Paleontology* 26(3, Supplement):118A.
- Seeley, H. G. 1887. On the classification of the fossil animals commonly named Dinosauria. *Proceedings of the Royal Society of London* 43:165–171.
- Sellwood, B. W., and P. J. Valdes. 2008. Jurassic climates. *Proceedings of the Geologists' Association* 119:5–17.
- Strong, M. 2005. Historical assessment of the Durham Downs Gas Field project Durham Downs District, Bungil Shire South Queensland; in ARCHAEO Cultural Heritage Services (ed.), Spring Gully Power Station Environmental Impact Statement, Appendix D2. Historical Assessment Report. Origin Energy Pty, Brisbane, 110 pp.
- Swarbrick, C. F. J., A. R. G. Gray, and N. F. Exon. 1973. Injune Creek Group—amendments and an addition to stratigraphic nomenclature in the Surat Basin. *Queensland Government Mining Journal* 74:57–63.
- Tang, F., X. Jing, X. Kang, and G. Zhang. 2001. [*Omeisaurus maoianus*—A Complete Sauropoda from Jingyan, Sichuan]. China Ocean Press, Beijing, 128 pp. [Chinese with English summary]
- Thulborn, R. A. 1985. *Rhoetosaurus brownii* Longman, 1926. The giant Queensland dinosaur; pp. 166–171 in P. Vickers-Rich and G. F. van Tets (eds.), Kadimakara: Extinct Vertebrates of Australia. Pioneer Design Studio, Melbourne.
- Thulborn, R. A. 1994. Ornithopod dinosaur tracks from the Lower Jurassic of Queensland. *Alcheringa* 18:247–258.
- Thulborn, R. A. 2000. Australia's earliest theropods: footprint evidence in the Ipswich coal measures (Upper Triassic) of Queensland. *Gaia* 15:301–311.
- Upchurch, P. 1995. The evolutionary history of sauropod dinosaurs. *Philosophical Transactions of the Royal Society of London, Series B* 349:365–390.
- Upchurch, P. 1998. The phylogenetic relationships of sauropod dinosaurs. *Zoological Journal of the Linnean Society* 124:43–103.
- Upchurch, P., P. M. Barrett, and P. Dodson. 2004a. Sauropoda; pp. 259–322 in D. B. Weishampel, P. Dodson, and H. Osmólska (eds.), *The Dinosauria*, 2nd edition. University of California Press, Berkeley, California.
- Upchurch, P., P. M. Barrett, and P. M. Galton. 2007. A phylogenetic analysis of basal sauropodomorph relationships: implications for the origin of sauropod dinosaurs. *Special Papers in Palaeontology* 77:57–90.
- Upchurch, P., Y. Tomida, and P. M. Barrett. 2004b. A new specimen of *Apatosaurus ajax* (Sauropoda: Diplodocidae) from the Morrison Formation (Upper Jurassic) of Wyoming, USA. *National Science Museum Monographs* 26:1–108.
- Whitlock, J. A., and J. D. Harris. 2010. The dentary of *Suuwassea emiliae* (Sauropoda: Diplodocoidea). *Journal of Vertebrate Paleontology* 30:1637–1641.
- Wild, R. 1978. Ein sauropoden-rest (Reptilia, Saurischia) aus dem Posidonienschifer (Lias, Toarcium) von Holzmaden. *Stuttgarter Beiträge zur Naturkunde Serie B (Geologie und Paläontologie)* 41:1–15.
- Wilson, J. A. 2002. Sauropod dinosaur phylogeny: critique and cladistic analysis. *Zoological Journal of the Linnean Society* 136:217–276.
- Wilson, J. A. 2005. Overview of sauropod phylogeny and evolution; pp. 15–49 in K. A. Curry Rogers and J. A. Wilson (eds.), *The Sauropods: Evolution and Paleobiology*. University of California Press, Berkeley, California.
- Wilson, J. A., and M. T. Carrano. 1999. Titanosaurs and the origin of “wide-gauge” trackways: a biomechanical and systematic perspective on sauropod locomotion. *Paleobiology* 25:252–267.
- Wilson, J. A., and P. C. Sereno. 1998. Early evolution and higher-level phylogeny of sauropod dinosaurs. *Society of Vertebrate Paleontology Memoir* 5:1–68.
- Wilson, J. A., and P. Upchurch. 2009. Redescription and reassessment of the phylogenetic affinities of *Euhelopus zdanskyi* (Dinosauria: Sauropoda) from the Early Cretaceous of China. *Journal of Systematic Palaeontology* 7:199–239.
- Wiman, C. 1929. Die Kreide-Dinosaurier aus Shantung. *Palaeontologia Sinica, (Series C)* 6:1–67.
- Yadagiri, P. 2001. The osteology of *Kotasaurus yamanpalliensis*, a sauropod dinosaur from the Early Jurassic Kota Formation of India. *Journal of Vertebrate Paleontology* 21:242–252.
- Yates, A. M., and J. W. Kitching. 2003. The earliest known sauropod dinosaur and the first steps towards sauropod locomotion. *Proceedings of the Royal Society of London, B* 270:1753–1758.
- You, H., F. Tang, and Z. Luo. 2003. A new basal titanosaur (Dinosauria: Sauropoda) from the Early Cretaceous of China. *Acta Geologica Sinica* 77:424–429.
- Young, C.-C., and X. Zhao. 1972. [*Mamenchisaurus hochuanensis*]. Institute of Vertebrate Paleontology and Paleoanthropology, Monographs Series A 8:1–30. [Chinese]
- Zhang, Y. 1988. [The Middle Jurassic Dinosaurian Fauna from Dashanpu, Zigong, Sichuan. III. The Sauropod Dinosaurs 1. *Shunosaurus*]. Sichuan Scientific and Technological Publishing House, Chengdu, Sichuan, 89 pp. [Chinese with English summary]

APPENDIX 1. Description of modifications to the character list and matrix of Harris (2006).

Deleted Characters

Character 307: “Ossified calcaneum: present (0); absent or unossified (1).” This character is rarely coded with confidence because the calcaneum is susceptible to taphonomic loss and/or lack of preservation, especially if it is ‘unossified’ (this is the derived state); the calcaneum is also readily misidentified due its indistinct morphology (Bonnan, 2000). Although some taxa can be scored based on the inference the calcaneum is unossified/lost, it is impossible to distinguish this scenario from when the element is not preserved at all (the character is based on absence of evidence). For future analyses, we consider it practical to present character information on the calcaneum in a ‘presence-of-observation’ format; for example, based upon morphology of calcaneal facet on the astragalus.

Character 309: “Posture of the metatarsus: bound (0); spreading (1).” Although unlikely to influence interrelationships among nested sauropods this character was omitted because it requires reconstruction and biomechanical interpretation of the metatarsus in order to form an inference regarding the derived trait; in contrast, all other characters are based on observation of measurements or presence/absence states from osteological data.

Characters 312 and 314: “Caudolateral projection of distal condyle of metatarsal I: absent (0); present (1)” and “Rugosities on distal parts of dorsolateral portions of bodies of metatarsals I–III: absent (0); present (1).” The first character (previously considered a uniting trait of diplodocoids) is variable in size and shape where present. First, it is difficult to apply a scorable demarcation between a series of strong crest-like projections to weaker tuberosities on the distolateral condyle of Mt I. Second, for tuberosities notable on Mt I, character 312 is repeat-coded in the matrix under character 314. We recode both into a new character (no. 333) below.

Additional Characters

Character 332: “Number of phalanges on pedal digit III: four or more (0); three or fewer (1).” Added to this study.

Character 333: “Distolateral projection on any or all bodies of metatarsals I–III: absent (0); present as simple rounded extensions (1); present on Mt I–III, and further developed on Mt I (compared to Mt II–III) as a well developed ‘lip’/crest often confluent with a fossa (2).” This character replaces omitted characters 312 and 314. Across the three states of character 333 we attempt to apply distinction in the level of development of the distolateral projection.

Emended and Recoded Characters

Character 300: “Morphology of the astragalus: rectangular (0); wedge-shaped (with reduced craniomedial corner) (1).” The character description does not designate an orientation, and given that the astragalus may be wedge-shaped in two views (cranially and proximally), it may be easily confused with character 301 (“Craniocaudal dimension of astragalus as seen in proximal view”). Character 300 is therefore reworded here to explicitly identify the trait in cranial view: “Morphology of astragalus in cranial view: rectangular (0); wedge-shaped, narrowing medially (1).”

Character 301: “Craniocaudal dimension of astragalus as seen in dorsal view: widens medially (0); narrows medially (1).”

The available states do not account for astragular shapes that do not change in width (i.e., are parallel craniocaudally). The plesiomorphic state is therefore reworded: “Craniocaudal dimension of astragalus as seen in dorsal view: widens medially or does not change in width (0); narrows medially (1).”

Character 308: “Ossified distal tarsals 3 and 4: present (0); absent or unossified (1).” This character suffers from similar problems to character 307 noted above, and we similarly suggest a recoding of it in future studies. Here, we retain rather than delete it because the record and distribution of distal tarsals in saurodromorphs is more complete and appears restricted to basal non-neosauropods, respectively, meaning it is scored with more confidence than character 307 is. For the present, we revise the character to “Ossified distal tarsals: present (0); absent or unossified; or unknown in near-complete articulated tarsoppedes (1).”

Character 330: “Development of pedal digit IV ungual: subequal in size to unguals of pedal digits II and III (0); rudimentary or absent (1).” The wording of this character does not allow for unguals that are smaller than the counterparts on digits II–III and are not ‘rudimentary’ (i.e., ungular or onychiform in morphology, as opposed to nubbin-shaped terminal phalanges). The coding of the character has been changed to accommodate all morphologies of the terminal phalanx of the digit: “Development of terminal phalanx of pedal digit IV: onychiform phalanx, greater than one-third size of terminal phalanges of pedal digits II–III (0); nubbin terminal phalanx (non-ungular) or ungual less than third size of terminal phalanx of either pedal digit II or III (1)”; several taxa have been re-scored for this character (below).

Re-scored Taxa, Resulting from Recoding of Above Characters and Additional Information (new scores for character states in parentheses)

Vulcanodon: 186(0); 252(0); 282(?) because the distal end of femur is incomplete for the proportional position of the fourth trochanter to be scored; 304(1) because the astragalus ascending process is deflected caudally to reach the caudal edge in *Vulcanodon* and *Tazoudasaurus* (Allain and Aquesbi, 2008); 330(?) because digit III is incomplete.

Shunosaurus: 291(1) based on Allain and Aquesbi (2008:character 179); 330(0); 331(1) because the spikes situated over the terminal caudal vertebrae in *Shunosaurus* (and in *Spinophorosaurus*) are dermal ossifications. Future analyses will require the coding of this character to discriminate between the fuller-bodied covering of osteoderms in titanosaurs from the spikes over the terminal tail in early gravisaurids.

Patagosaurus: 279(0).

Omeisaurus: 301([0+1]→0) due to the above recoding of this character; 316(2→1) because the metatarsal/tibia ratio is greater than that prescribed for state 2.

Mamenchisaurus: 123(1); 124(1); both scores based on data from *M. youngi* (Ouyang and Ye, 2002).

Suuwassea: Seven characters listed in Whitlock and Harris (2010:table 1) are re-scored.

Barapasaurus: New information (Bandyopadhyay et al., 2010) allow many characters to be re-scored for Harris’ matrix, so the entire submatrix is listed. Other adjustments are: 314(?); 325(?) because the pedal data is based on unassociated bones; 329(?) because no unguals of pedal digits II–III are preserved. Character 290 is based on associated ‘skeleton C’ (Bandyopadhyay et al., 2010). Emended character-state matrix for *Barapasaurus*:

???????????	???????????	???????????	???????????
???????????	???????????	???????????	???????????
???????????	??????110	??1??1000	0?0010?000
?111?0200	0100?01?11	0000102000	0001011001
?0?0?0?0?0	??????0?1	00????10?0	000?????0?
2?00??010?	0000?10000	???001001	0011?110?0
00???????	011????010	0110101010	0010100111
0021011001	0010111111	??1?110?0	10111?1???
????????1??	0?1		

Character States of New Taxa Added to the Modified Harris Matrix (deleted characters also listed)

Tazoudasaurus

0???????????	???????????	?????0?00?0	?0?????1??
??00?????0	-??????????	??0???????	??1?????10
100100??1	?0?11?0110	?010??1000	01?010??00
?11000100	0000-01-11	?02011?000	00010?????
?0?????000	?00001?01	000?00000	?000?0?0?
2001?1????	??????00?0	???001001	0011110?1
000101??00	00110101??	001??00000	?01??0?1?1
011101100?	0000111111	??111??00	?000?????0
00?01?100	??0		

Spinophorosaurus

1??1???????	??????????1	???00?2011	101??0?1?0
1?????????0	-??????????	0?0??01000	01100?????0
1?11???????	?11????110	?01?4?100?	010010?000
?211?0?0?0	??????1?11	0??000?000	0??10?????
?0??1??0?0	0?00000???	000?000???	0000100?00
2001?1011?	0000??00?0	???0?1001	001???????
???????????	????????1??	??1??00010	?01??00?10
1111010001	00001?111?	1?1000????	???????????
???????????	1??		

Rhoetosaurus

???????????	???????????	???????????	???????????
???????????	???????????	???????????	???????????
???????????	???????????	??????120?	?0?????????
?11?1/20???	??????1?1?	0??1?0??1	00??1????1
?000??1?00	0100001???	0?0000?00?	???????????
2???????????	???????????	???????????	???????????
???????????	???????????	?????0?0??	?????????111
112101????	011011?011	10?001??11	1111110?11
1111111110	0?1		